AD

USAAVLABS TECHNICAL REPORT 68-49B

AN INVESTIGATION OF THE DYNAMIC STABILITY CHARACTERISTICS OF A QUAD CONFIGURATION, DUCTED-PROPELLER V/STOL MODEL

VOLUME II

PHASE II - LONGITUDINAL DYNAMICS AT HIGH DUCT INCIDENCE DATA REPORT

By

William F. Putman
Joseph J. Traybar
Howard C. Curtiss, Jr.
John P. Kuhn

August 1968

U. S. ARMY AVIATION MATERIEL LABORATORIES
FORT EUSTIS, VIRGINIA

CONTRACT DAAJ02-67-C-0025
PRINCETON UNIVERSITY
PRINCETON, NEW JERSEY

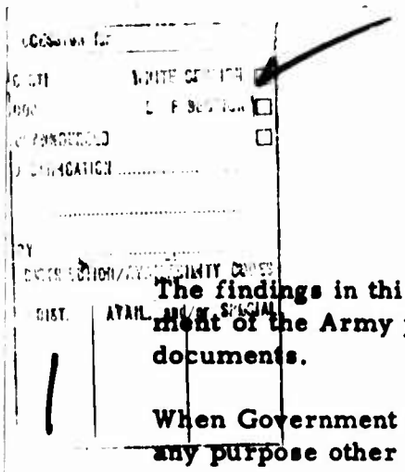

Disclaimers

The findings in this report are not to be construed as an official Department of the Army position unless so designated by other authorized documents.

When Government drawings, specifications, or other data are used for any purpose other than in connection with a definitely related Government procurement operation, the United States Government thereby incurs no responsibility nor any obligation whatsoever; and the fact that the Government may have formulated, furnished, or in any way supplied the said drawings, specifications, or other data is not to be regarded by implication or otherwise as in any manner licensing the holder or any other person or corporation, or conveying any rights or permission, to manufacture, use, or sell any patented invention that may in any way be related thereto.

Disposition Instructions

Destroy this report when no longer needed. Do not return it to the originator.

DEPARTMENT OF THE ARMY
U. S. ARMY AVIATION MATERIEL LABORATORIES
FORT EUSTIS, VIRGINIA 23604

This report has been reviewed by the U. S. Army Aviation Materiel Laboratories, the Naval Air Systems Command, and the Air Force Flight Dynamics Laboratories. It is considered to be technically sound.

This work, which was performed under Contract DAAJ02-67-C-0025, was undertaken to determine experimentally the longitudinal dynamic stability characteristics of a quad configuration, four-duct V/STOL aircraft similar to the X-22A configuration at four low-speed/high-duct incidence trim conditions. The data presented include time histories of the model motions in various longitudinal degrees of freedom that occur when the model is disturbed from trimmed flight. The Princeton Dynamic Model Track was utilized to perform the investigation.

This report is published for the exchange of information and the stimulation of ideas.

Task 1F162204A14233
Contract DAAJ02-67-C-0025
USAAVLABS Technical Report 68-49B
August 1968

AN INVESTIGATION OF THE DYNAMIC STABILITY CHARACTERISTICS OF A QUAD CONFIGURATION, DUCTED-PROPELLER V/STOL MODEL

Volume II

Phase II - Longitudinal Dynamics at High Duct Incidence
Data Report

Aerospace Sciences Report 836

By

William F. Putman
Joseph J. Traybar
Howard C. Curtiss, Jr.
John P. Kukon

Prepared by

Department of Aerospace and Mechanical Sciences
Princeton University
Princeton, New Jersey

for

U. S. ARMY AVIATION MATERIEL LABORATORIES
FORT EUSTIS, VIRGINIA

SUMMARY

The results of experiments to determine the longitudinal dynamic stability characteristics of a quad configuration, ducted-propeller V/STOL aircraft at four low-speed/high-duct-incidence trim conditions (i_d = 80° , 70° , 60° , and 50°) are presented. Longitudinal transient responses in various degrees of freedom were measured using a dynamic model on the Princeton Dynamic Model Track. The data presented include time histories of the model motions in various longitudinal degrees of freedom that occur when the model is disturbed from trimmed flight. Responses are presented both with and without pitch rate feedback.

The dynamic model employed in these experiments is a generalized research model arranged to represent closely the Bell X-22A V/STOL aircraft.

The data presented in this report comprise the second phase of a three-phase investigation of the dynamic stability characteristics of a quad configuration, ducted-propeller V/STOL aircraft at low speeds and high duct incidences. The other two phases pertain to the lateral and longitudinal hovering stability characteristics, presented in Reference 1, and the lateral/directional characteristics at the same trim conditions as presented here.

FOREWORD

This research was performed by the Department of Aerospace and Mechanical Sciences, Princeton University, under the sponsorship of the United States Army Aviation Materiel Laboratories Contract DAAJ02-67-C-0025, with financial support from the United States Naval Air Systems Command and the Air Force Flight Dynamics Laboratory. The research was monitored by Mr. Robert P. Smith of the United States Army Aviation Materiel Laboratories.

The research was directed by Associate Professor H. C. Curtiss, Jr., and was conducted by Messrs. W. F. Putman, J. J. Traybar, and J. P. Kukon, all of Princeton University.

TABLE OF CONTENTS

LIST OF ILLUSTRATIONS

LIST OF SYMBOLS

b	propeller blade chord, feet
c	duct chord, feet
cg	center of gravity of pivoting mass of model
d	propeller blade diameter, feet
FS	fuselage station (horizontal reference), inches
g	acceleration due to gravity, feet per second squared
h	altitude, feet
I_y	model moment of inertia in pitch about pivot axis, slug-feet squared
i_d	duct incidence, degrees
$K_{\dot{\theta}}$	feedback gain, proportionality constant between differential blade angle change and angular velocity in pitch, seconds
k_{θ_m}	mechanical spring constant, foot-pounds per radian
M_u, M_w, $M_{\dot{w}}$, $M_{\dot{\theta}}$	stability derivatives, rate of change of pitching moment divided by inertia I_y with variable indicated in subscript
$M_{\Delta\beta_{PITCH}}$	longitudinal control effectiveness, rate of change of pitching moment divided by inertia I_y with propeller differential collective pitch, per second squared
$\bar{M}_{\dot{\theta}}$	augmented pitch damping stability derivative ($\bar{M}_{\dot{\theta}} = M_{\dot{\theta}} + K_{\dot{\theta}} M_{\Delta\beta_{PITCH}}$), per second
m	mass accelerated by the model when translating vertically, slugs ($m = m_p + m_v = 1.60$ slugs)
m_h	mass of horizontal travel link, slugs ($m_h = 0.11$ slugs)
m_p	pivoting mass of model, slugs ($m_p = 1.48$ slugs)

m_t	total mass accelerated by the model when translating horizontally, slugs ($m_t = m + m_h + 1.71$ slugs)
$\frac{m}{m_t}$	ratio of vertical to horizontal masses ($\frac{m}{m_t} = 0.936$)
m_v	mass of vertical travel link, slugs ($m_v = 0.12$ slugs)
R	propeller blade radius, feet
r	distance along propeller radius (measured from axis of rotation), feet
$\frac{r}{R}$	propeller blade radial station
rpm	model propeller rotational speed, revolutions per minute
t	propeller blade thickness, feet
U	aircraft velocity along body-fixed X axis (stability axis system), feet per second ($U = U_o + u$)
U_f	aircraft horizontal velocity (space-fixed axis system), feet per second ($U_f = U_{o_f} + u_f$)
U_o	aircraft initial velocity along flight path (stability axis system), feet per second
U_{o_f}	aircraft initial horizontal velocity (space-fixed axis system), feet per second
u	aircraft perturbation velocity along body-fixed longitudinal axis (stability axis system), feet per second
u_f	aircraft horizontal perturbation velocity (space-fixed axis system), feet per second
W_f	aircraft vertical velocity (space-fixed axis system), feet per second ($W_f = W_{o_f} + w_f$)
W_{o_f}	aircraft initial vertical velocity (space-fixed axis system), feet per second
W_p	model pivoting weight, pounds ($W_p = 47.5$ pounds)

w	aircraft perturbation velocity along body-fixed Z axis (stability axis system), feet per second
w_f	aircraft vertical perturbation velocity (space-fixed axis system), feet per second
WL	fuselage water line (vertical reference station), inches
X	body-fixed longitudinal axis, initially aligned into the relative wind (stability axis system)
X_f	horizontal axis (space-fixed axis system)
X'	perturbed location of X_f
X_u, X_w, $X_{\dot{\theta}}$ Z_u, Z_w, $Z_{\dot{\theta}}$	stability derivatives, rate of change of aerodynamic force divided by the mass m with variable indicated in subscript
x_{cg}	longitudinal distance of cg from pivot axis, inches
x_{PIVOT}	longitudinal position of model pivot axis referenced to FS 0, inches (model scale unless noted)
$\bar{x}$	axial distance (coordinate) from duct leading edge, inches (full scale)
Y_f	lateral axis (space-fixed axis system)
Y'	perturbed location of Y_f
$\bar{y}$	radial distance (coordinate) from duct center line, inches (full scale)
Z	body-fixed vertical axis, initially aligned perpendicular to the relative wind in the vertical plane (stability axis system)
Z_f	vertical axis (space-fixed axis system), aligned with g
Z'	perturbed location of Z_f
z_{cg}	vertical distance of cg from pivot axis, inches
z_{PIVOT}	vertical position of model pivot axis referenced to WL 0, inches (model scale unless noted)

β local propeller blade angle, degrees

β_F average propeller blade angle on the two front propellers, degrees

β_R average propeller blade angle on the two rear propellers, degrees

$\beta_{.75R}$ average propeller blade angle required for vertical force trim (collective pitch) measured at the three-quarter radius and averaged for four propellers, degrees

$\Delta M_{\dot{u}_{cg}}$ additional stability derivative due to vertical displacement of cg from pivot axis, per foot $\left(\Delta M_{\dot{u}_{cg}} = - \frac{m_p z_{cg}}{I_y}\right)$

$\Delta M_{\dot{w}_{cg}}$ additional stability derivative due to horizontal displacement of cg from pivot axis, per foot $\left(\Delta M_{\dot{w}_{cg}} = \frac{m_p x_{cg}}{I_y}\right)$

$\Delta M_{\theta_{cg}}$ additional stability derivative due to vertical displacement of cg from pivot axis, per second squared $\left(\Delta M_{\theta_{cg}} = - \frac{W_p z_{cg}}{I_y}\right)$

ΔM_{θ_m} additional stability derivative due to mechanical spring, per second squared $\left(\Delta M_{\theta_m} = - \frac{k_{\theta_m}}{I_y}\right)$

$\Delta\beta$ change in propeller blade angle, degrees (positive for trailing edge down with duct at 90° incidence)

$\Delta\beta_o$ longitudinal control required for pitching moment trim (differential collective pitch), degrees or radians $\left(\Delta\beta_o = \frac{\beta_R - \beta_F}{2}\right)$

$\Delta\beta_{PITCH}$ longitudinal control input due to stability augmentation, degrees $\left(\Delta\beta_{PITCH} = \frac{\Delta\beta_{RS} + \Delta\beta_{RP}}{4} - \frac{\Delta\beta_{FS} + \Delta\beta_{FP}}{4}\right)$

δ elevon deflection, degrees (positive for trailing edge forward with duct at 90° incidence)

θ fuselage pitch angle, degrees or radians (positive nose up)

λ_L	linear scale factor $\lambda_L = \frac{\text{model length}}{\text{full-scale length}}$
$(\dot{\ })$	differentiation with respect to time
$(\ )_{FP}$	control deflection associated with front port duct
$(\ )_{FS}$	control deflection associated with front starboard duct
$(\ )_{RP}$	control deflection associated with rear port duct
$(\ )_{RS}$	control deflection associated with rear starboard duct

INTRODUCTION

A series of experiments to determine the longitudinal dynamic stability characteristics of a quad configuration, ducted-propeller V/STOL aircraft at low speeds and high duct incidences were conducted on the Princeton Dynamic Model Track. The data presented in this report from Phase II of a three-part investigation, consist of measurement of the longitudinal transient response characteristics of a dynamic model at four low-speed trim conditions in transition flight. Reference 1 presents experimental data from Phase I, an investigation of the hovering stability characteristics, and a succeeding report will present data from Phase III, concerned with the lateral/directional dynamics at the same trim conditions as those of Phase II.

The dynamic model employed in these tests is shown in Figure 1. The model, described in Reference 2, was designed as a general research model with variable geometry and lifting system configuration such that a variety of quad V/STOL designs could be simulated. In the configuration selected for the tests described here, the model closely resembles a 0.145-scale dynamic model of the Bell X-22A V/STOL research aircraft. The model differs from actual aircraft (as given in Reference 3) in certain minor details which are described in the section entitled Description of Apparatus under Model.

The test program consisted of measurement of the transient response characteristics of the dynamic model in various longitudinal degrees of freedom when disturbed from trimmed level flight. One of the features of the Princeton Dynamic Model Track (described in detail in Reference 4) is the ability to use the servo carriage to restrict the degrees of freedom of the model such that response measurements can be conducted in various combinations of degrees of freedom as well as the three-degree-of-freedom longitudinal motion. These restricted degree-of-freedom tests greatly assist in the analysis of the data for stability derivatives of the vehicle. Therefore, response measurements in this investigation included three-degree-of-freedom experiments (pitch angle/horizontal velocity/vertical velocity), two-degree-of-freedom measurements (pitch angle/horizontal velocity and pitch angle/vertical velocity), and single-degree-of-freedom measurements (pitch angle only). The single-degree-of-freedom measurements are particularly useful for a direct determination of the angular damping of the vehicle.

In addition to the time histories of the basic model, data were taken with various levels of pitch rate feedback. Differential propeller blade angle on the fore-and-aft ducts proportional to the angular velocity of the model in pitch was used where noted in the data. Transient response measurements with stability augmentation are valuable for determination of the stability derivatives of the model. This is particularly true when the basic model is markedly unstable. A longer time history can be obtained in the augmented case, permitting more accurate determination of the transient characteristics. The test conditions covered are given in

Table I.

All data are presented in model scale and may be interpreted in terms of the full-scale vehicle, (which the model closely resembles) using the conversion factors given in Table II.

DESCRIPTION OF APPARATUS

TEST FACILITY

The Princeton University Dynamic Model Track is a facility designed expressly for the study of the dynamic motions of helicopter and V/STOL models at equivalent flight speeds of up to 60 knots (for a one-tenth scale model). Basic components of the facility include a servo-driven carriage riding on a track 750 feet long, located in a building with a cross section of 30 by 30 feet; the carriage has an acceleration potential of 0.6g and a maximum speed of 40 feet per second. A detailed description of the facility and the testing techniques employed may be found in Reference 4.

A model can be attached to the carriage by one of several booms. The mount used to conduct longitudinal investigations is shown in Figure 1. This mount permits relative displacements of the model with respect to the carriage in horizontal and vertical directions. The model is supported on a three-axis gimbal system that allows selection of any or all of the three angular degrees of freedom. Horizontal relative motion of the model with respect to the carriage is sensed and used to command the carriage to follow the model in a closed-loop fashion. Similarly, vertical displacement of the model with respect to the carriage commands the boom to move vertically. This servo operation of the carriage allows the model to fly "free", with no restraints on the dynamic motions being investigated. This method of testing may be considered to be similar to dynamic flight testing, but considerably more control over the experiment is possible.

The dynamic tests conducted during this program included one-, two-, and three-degree-of-freedom motion measurements. The model was mounted as shown in Figure 1. The transient behavior of the model was dominated in general by an unstable oscillation, except at the lowest duct incidence investigated ($i_d = 50^\circ$), so only in this latter case were predetermined control inputs used to excite the model motions.

MODEL

A photograph of the model is shown in Figure 2, and a three-view drawing is presented in Figure 3. The model's pertinent dimensions and inertia characteristics are listed in Table III and the model Reference Stations are defined and compared with full-scale X-22A Reference Stations in Figure 4. The model was designed as a general research model for investigation of the dynamic stability characteristics of various quad configuration V/STOL aircraft as described in Reference 2; however, the configuration selected for these tests matched as closely as possible the Bell X-22A configuration.

This dynamic model is powered by a 200-volt, 400-cycle, 3-phase electric motor. The motor drives the four ducted propellers through a central

transmission and various right-angle gearboxes. The aerodynamic shape of the model is obtained through the use of a Fiberglas skin with Styrofoam stiffeners. The propeller blades are made with a plastic foam core and Fiberglas skin. The geometric characteristics of the propeller are shown in Figure 5, and the duct geometry is shown in Figure 6. The duct shape is identical to that of the Bell X-22A aircraft.

Model control positions are set from a control console on the carriage. The blade pitch angles on each of the four propellers are electrically controllable. Also, the deflection angles of the elevons are electrically controllable. All of these control systems are closed-loop position controls and are used as such in the portions of the experiments involving feedback to alter the transient motions of the model. The dynamic characteristics of these feedback loops are such that the time response of the controls is negligible in the frequency range of interest. Although the control servo loops are nonlinear, using polarized relays for power amplification, they can be characterized as having a closed-loop natural frequency of approximately 10 cycles per second with a damping ratio of approximately seven-tenths. The servo gear ratios were selected so that the rate limits arising from the rpm limitations of the control drive motors were equal to or greater than scaled rate limits determined from full-scale Bell X-22A values.

This research model differs from the Bell X-22A in the following particulars:

1. The elevon on the model differs from that on the full-scale aircraft. The model elevon has no movable surface forward of the hinge line, and its hinge line is located below the trailing edge of the duct as shown in Figure 7. While these differences would affect the control effectiveness and the control loads, they would not be expected to have any significant effect on the dynamic motions.

2. The duct rotation point is at a different location on the model (84 percent c) than on the full-scale aircraft (55 percent c).

   With the ducts at 90 degrees incidence, the propeller hubs are in the same relative position on the model as on the full-scale aircraft. The center of gravity of the model is higher (by 1.2 percent c) on the model with respect to the propeller hubs than on the full-scale aircraft.

3. For the tests at duct incidences of 80 degrees and 70 degrees the vertical tail on the model was smaller than on the full-scale vehicle as shown in Figure 3. At duct incidences of 60 degrees and 50 degrees, the model vertical tail was the larger scaled size as indicated on the same figure.

This model was planned as a general research model; numerous other quad configuration layouts can be simulated through the use of interchangeable

parts as described in Reference 2. No attempt was made in the design stage to simulate the X-22A precisely. However, the modifications above will not result in appreciable differences in the model dynamic stability characteristics.

EXPERIMENTAL RESULTS AND DISCUSSION

The experimentally determined trim conditions are shown in Figure 8 as graphs of trim velocity U_f and average propeller pitch $\beta_{.75R}$ as a function of duct incidence. The elevons were set at zero deflection angle for all tests. All experiments were conducted with a model weight of 51.5 pounds, corresponding to a full-scale vehicle gross weight of 16,700 pounds. Due to the large pitching moments developed by the model in some of the flight conditions encountered, it was considered to be desirable to move the center of gravity of the model as indicated in Table III, such that excessive levels of differential propeller blade angle (differential collective pitch) would not be required for trim. The differential collective pitch $\Delta\beta_o$ required for trim is given in Table I.

Transient response characteristics are presented about a space-fixed axis system as shown in Figure 9 and further discussed in Appendix I. Time histories of the longitudinal transient responses of the quad configuration V/STOL aircraft model from the level flight trim conditions at four duct incidences ($i_d = 80^\circ$, 70°, 60°, and 50°) are presented in Figures 10 through 37.

The responses shown include one-, two-, and three-degree-of-freedom time histories as discussed previously. The single-degree-of-freedom responses are presented to permit a direct determination of the angular damping characteristics of the model. These runs are presented in Figures 10, 17, 29, and 34. With the exception of the runs presented in Figure 34 ($i_d = 50^\circ$), mechanical springs have been added to the model to provide a restoring moment about the model pitch axis such that the single-degree-of-freedom motions will be oscillatory. In this way the time histories are more readily analyzed for angular damping derivatives. Mechanical springs were not necessary in the $i_d = 50^\circ$ case since sufficient aerodynamic spring M_w was present to make the response oscillatory. The angular spring constant and the inertia of the model are given in Table III. Data are presented with the model motor off and the rpm equal to zero so that the mechanical damping of the model mounting system may be determined. This damping, due to friction, should be subtracted from the damping measured with the model running to determine the aerodynamic damping. It may be noted that the mechanical damping is very small compared to the total damping with the model running.

These data include runs showing the transient motion of the basic model as well as the transient motion with various levels of rate feedback. As mentioned earlier, the dynamic characteristics of the model control system are such that the control system transfer function may be considered to be equal to unity over the frequency range of interest here.

The general trend of the stability characteristics measured is to show a transient response in three degrees of freedom that is dominated by an

unstable oscillation. The instability becomes less severe as the duct incidence is reduced, ultimately becoming stable at a duct incidence of 50 degrees. At the lowest duct incidence, control inputs were used to excite the transient motion of the model. At the other three duct incidences tested, the model motions were self-excited. In this way a maximum length time history is obtained.

TABLE I. SUMMARY OF TEST CONDITIONS

All tests conducted at model lift = weight = 51.5 lb
(This is equivalent to 14,800 lb full scale flying at a 4200-ft pressure altitude.)

Duct Incidence i_d (deg)	Average Propeller Pitch $\beta_{.75R}$ (deg)	Differential Collective Pitch $\Delta\beta_o$ (deg)	Propeller Speed (rpm)	Trim Velocity U_{o_f} (ft/sec)	Degrees of Freedom	Stability Augmentation $K_{\dot{\theta}}$ (sec)	Run Nos.	Fig. Nos.
80	25.2	1.9	0	0	θ*,**	none	1282	10
			6780	11	θ*	none	1286	
				8	θ-U_f	none	843 847	11
				11	θ-U_f	0.030	854 856	12
				11	θ-U_f	0.044	862	13
				11	θ-U_f	0.060	863	14
	23.7	1.8	6780	11	θ-w_f	none	908	15
				11	θ-U_f-w_f	none	906 907	16

*θ Freedom restrained with mechanical spring. See Table III for spring rate.
**Model cg at pivot. See Table III for I_y.

TABLE I - Continued

All tests conducted at model lift = weight = 51.5 lb

(This is equivalent to 14,800 lb full scale flying at a 4200-ft pressure altitude.)

Duct Incidence i_d (deg)	Average Propeller Pitch $\beta_{.75R}$ (deg)	Differential Collective Pitch $\Delta\beta_o$ (deg)	Propeller Speed (rpm)	Trim Velocity U_{o_f} (ft/sec)	Degrees of Freedom	Stability Augmentation $K_{\dot{\theta}}$ (sec)	Run Nos.	Fig. Nos.
70	25.2	2.8	0	0	θ*,**	none	1271 1272	17 & 17 Concl.
			6780	22	θ*	none	1270 1275	
	26.2	6.0	6780	22	θ-U_f	none	931 933	18
					θ-U_f	0.021	968 969	19
					θ-U_f	0.027	961	20
					θ-U_f	0.030	960	21
					θ-U_f	0.044	957	22
					θ-U_f	0.060	955	23
					θ-w_f	none	991 995	24
					θ-U_f-w_f	none	990	25
					θ-U_f-w_f	0.021	985	26
					θ-U_f-w_f	0.027	984	27
					θ-U_f-w_f	0.030	980	28

TABLE I - Continued

All tests conducted at model lift = weight = 51.5 lb

(This is equivalent to 14,800 lb full scale flying at a 4200-ft pressure altitude.)

Duct Incidence i_d (deg)	Average Propeller Pitch $\beta_{.75R}$ (deg)	Differential Collective Pitch $\Delta\beta_o$ (deg)	Propeller Speed (rpm)	Trim Velocity U_{o_f} (ft/sec)	Degrees of Freedom	Stability Augmentation $F_{\dot{\theta}}$ (sec)	Run. Nos.	Fig. Nos.
60	25.5	4.1	0	0	θ*,**	none	1276	29
			6780	28	θ*	none	1280	
	25.4	2.1	6780	28	θ-U_f	none	1045 1047	30
					θ-U_f	0.027	1032	31
					θ-w_f	none	1062 1065	32
					θ-U_f-w_f	none	1055	33
50	25.3	2.5	6780	36	θ***	none	1230 1232	34
					θ-U_f	none	1084	35
					θ-w_f	none	1112	36
					θ-U_f-w_f	none	1105 1109	37

***No mechanical spring in θ freedom.

TABLE II. SCALE FACTORS FOR DYNAMIC MODEL SIMILARITY

Multiply full-scale property by scale factor to obtain model property.

		For $\lambda_L = 0.1453$
Linear dimension	λ_L	0.1453
Area	λ_L^2	2.112×10^{-2}
Volume, mass, force	λ_L^3	3.071×10^{-3}
Moment	λ_L^4	4.463×10^{-4}
Moment of inertia	λ_L^5	6.487×10^{-5}
Linear velocity	$\lambda_L^{0.5}$	0.3812
Linear acceleration	λ_L^0	1.000
Angular velocity	$\lambda_L^{-0.5}$	2.623
Angular acceleration	λ_L	0.1453
Time	$\lambda_L^{0.5}$	0.3812
Frequency	$\lambda_L^{-0.5}$	2.623
Reynolds number	$\lambda_L^{1.5}$	5.541×10^{-2}
Mach number	$\lambda_L^{0.5}$	0.3812

where $\lambda_L = \dfrac{\text{model linear dimension}}{\text{full-scale linear dimension}}$

TABLE III. MODEL GEOMETRIC AND INERTIAL CHARACTERISTICS

Model Weight = 51.5 lb

Duct Incidence i_d (deg)	Pivot Axis Location		Location of cg Relative to Pivot		Moment of Inertia About Pivot Axis I_y (slug-ft^2)	Mechanical Spring Rate k_{θ_m} $\left(\frac{\text{ft-lb}}{\text{rad}}\right)$	Run Nos.	Fig. Nos.
	x_{PIVOT} (FS)	z_{PIVOT} (WL)	x_{cg} (in.)	z_{cg} (in.)				
80	45.70	20.10	0	0	2.82	18.1	1282	10
			2.47	0.37	2.44	18.1	1286	
	44.45	20.10	0	0	2.25	none	all	11-16
70	45.70	20.10	0	0.48	2.80	18.1	1272	17
						62.8	1271	
			2.55	0.48	2.15	18.1	1275	
						62.8	1270	
	44.45	20.10	0	0	2.23	none	all	18-28
60	45.70	20.10	0	0.60	3.17	18.1	1276	29
			2.47	0.60	2.63	18.1	1280	
						none	all	30-33
50	45.70	20.10	2.56	0.67	2.63	none	all	34-37

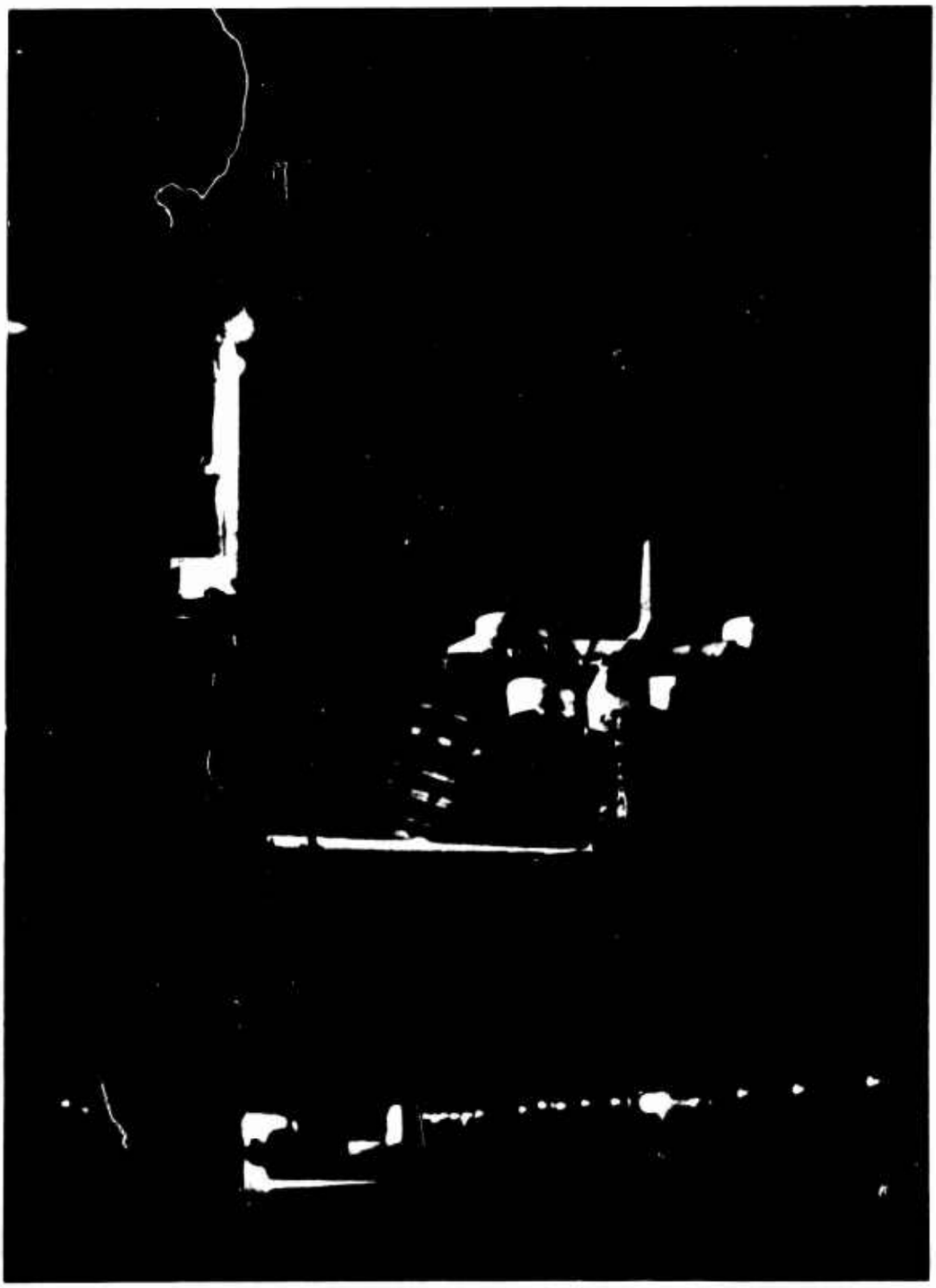

Figure 1. Photograph of Princeton Dynamic Model Track Showing Model Mounted on Longitudinal Dynamic Testing Apparatus.

Figure 2. Photograph of 0.145-Scale Quad Configuration Dynamic Model.

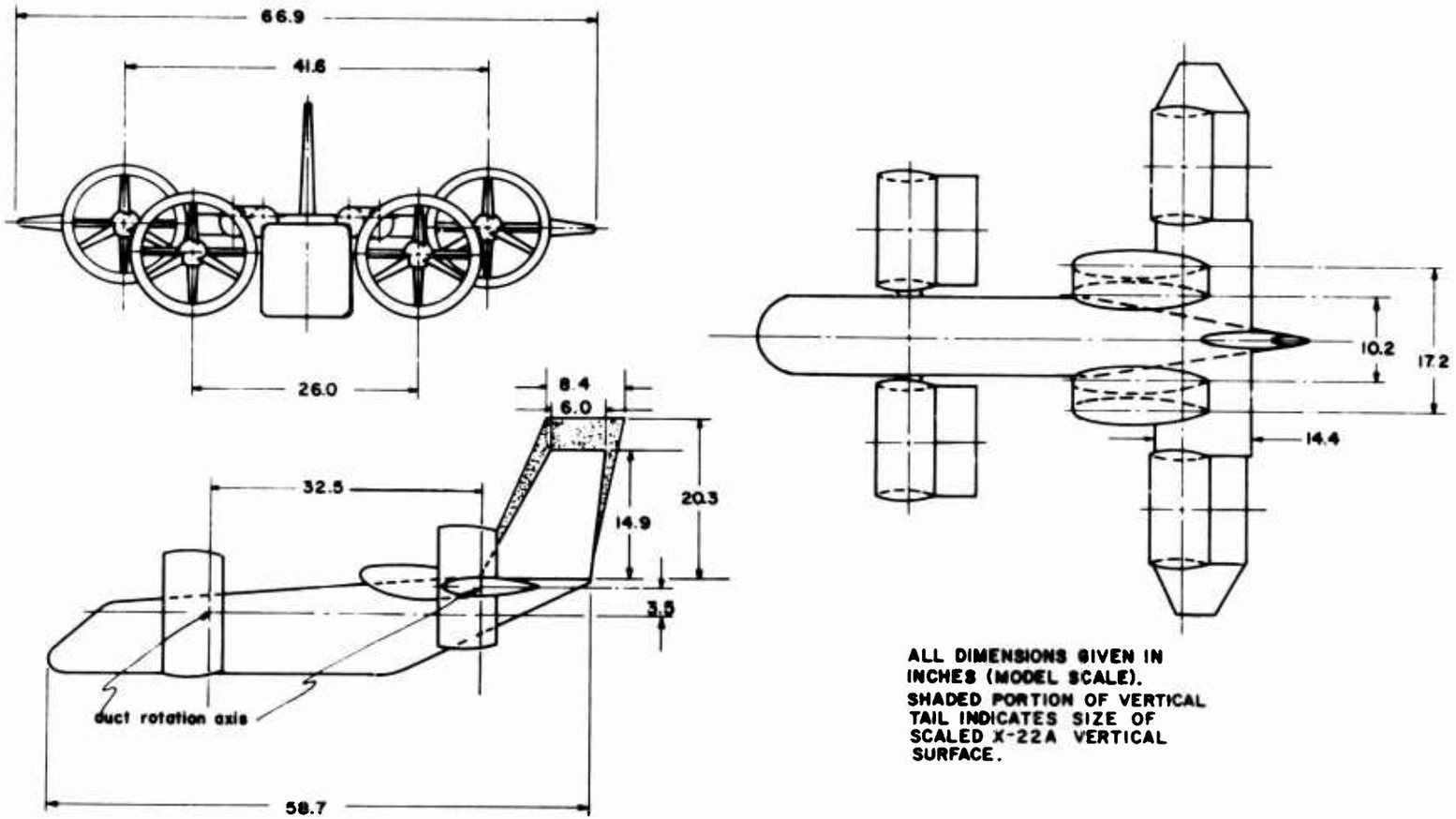

Figure 3. General Arrangement, Quad Configuration Dynamic Model.

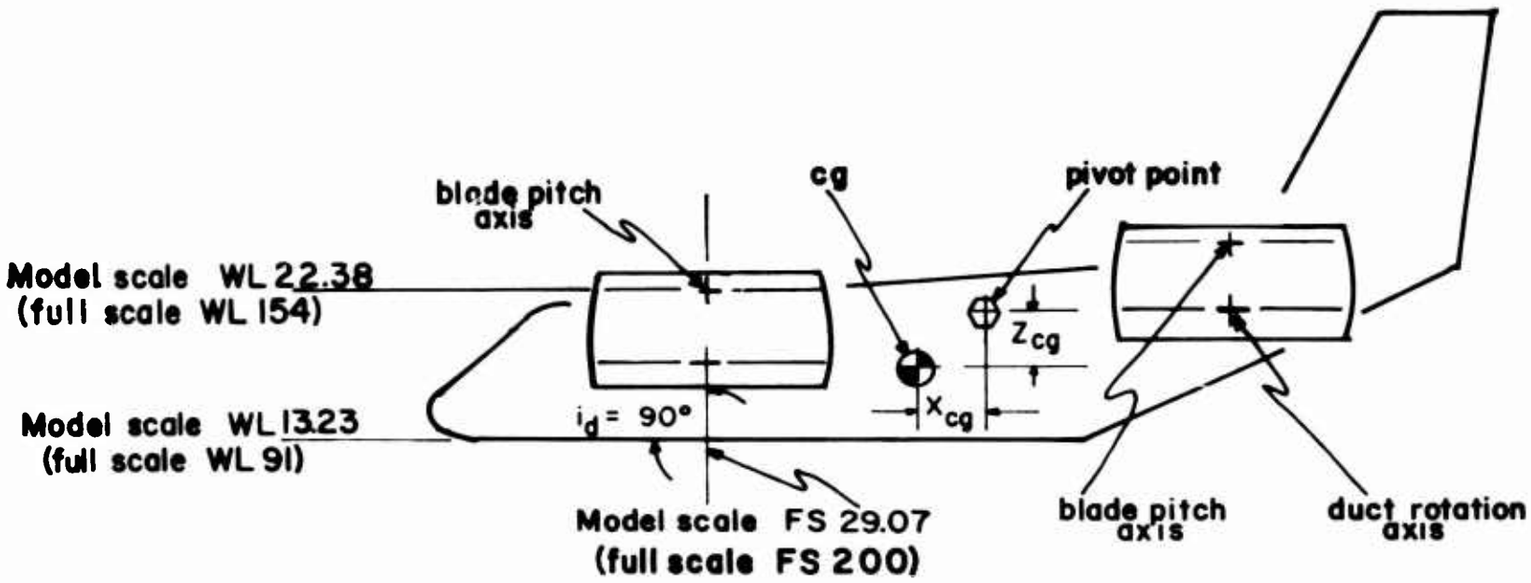

Note: 1.) Reference FS and WL locations shown do not change with duct rotation.

2) Pivot point is reference point for aerodynamic measurements of complete aircraft.

3) Model angular motions measured about pivot point.

Figure 4. Location of Model Reference Stations and cg.

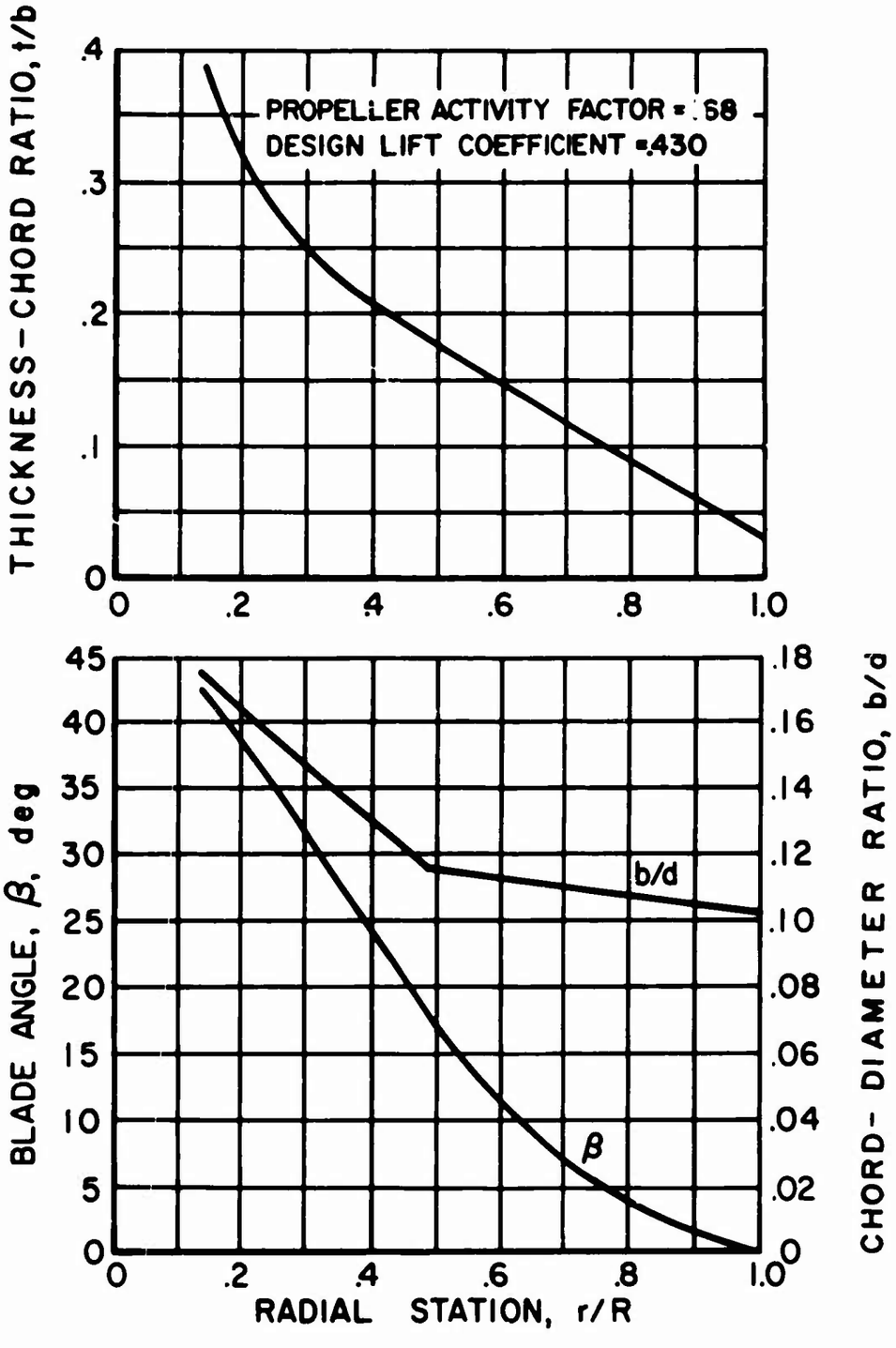

Figure 5. Geometric Characteristics of Three-Bladed Model Propellers.

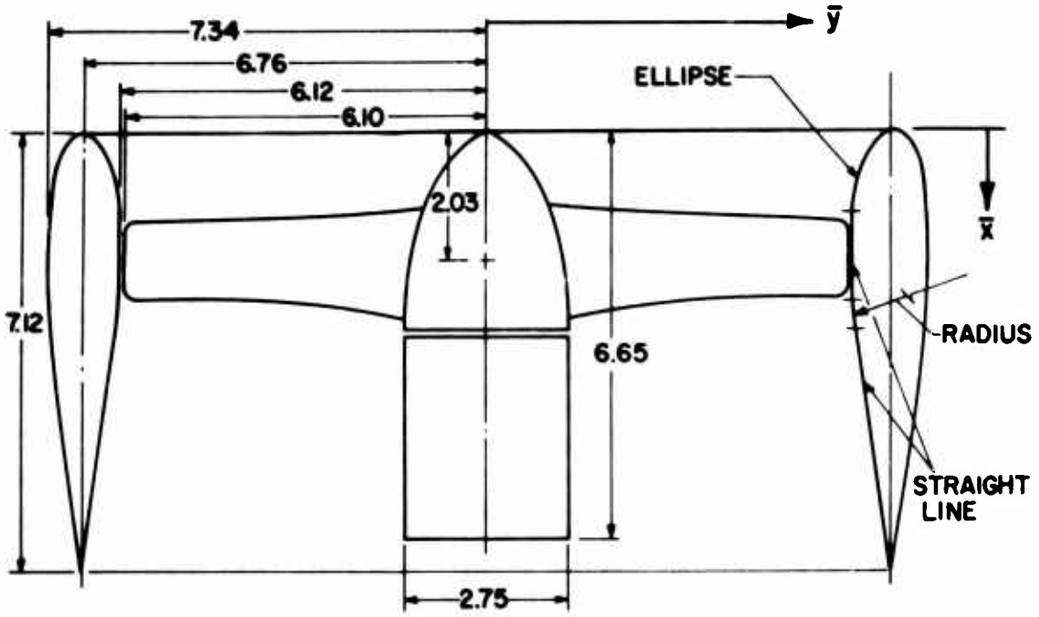

ALL DIMENSIONS ON ABOVE DRAWING IN INCHES (MODEL SCALE)

X-22A DUCT OUTER ORDINATES (FULL SCALE)	
x̄	ȳ
0	47.625
0.613	48.695
1.225	49.096
2.450	49.609
3.675	49.953
4.900	50.205
7.350	50.535
9.800	50.710
10.250	—
12.250	50.779
14.700	50.763
17.750	—
19.600	50.552
23.700	—
24.500	50.164
29.400	49.649
34.300	49.038
39.200	48.344
44.100	47.576
46.550	47.160
49.000	46.722

Figure 6. Geometric Characteristics of Scaled Model Ducts.

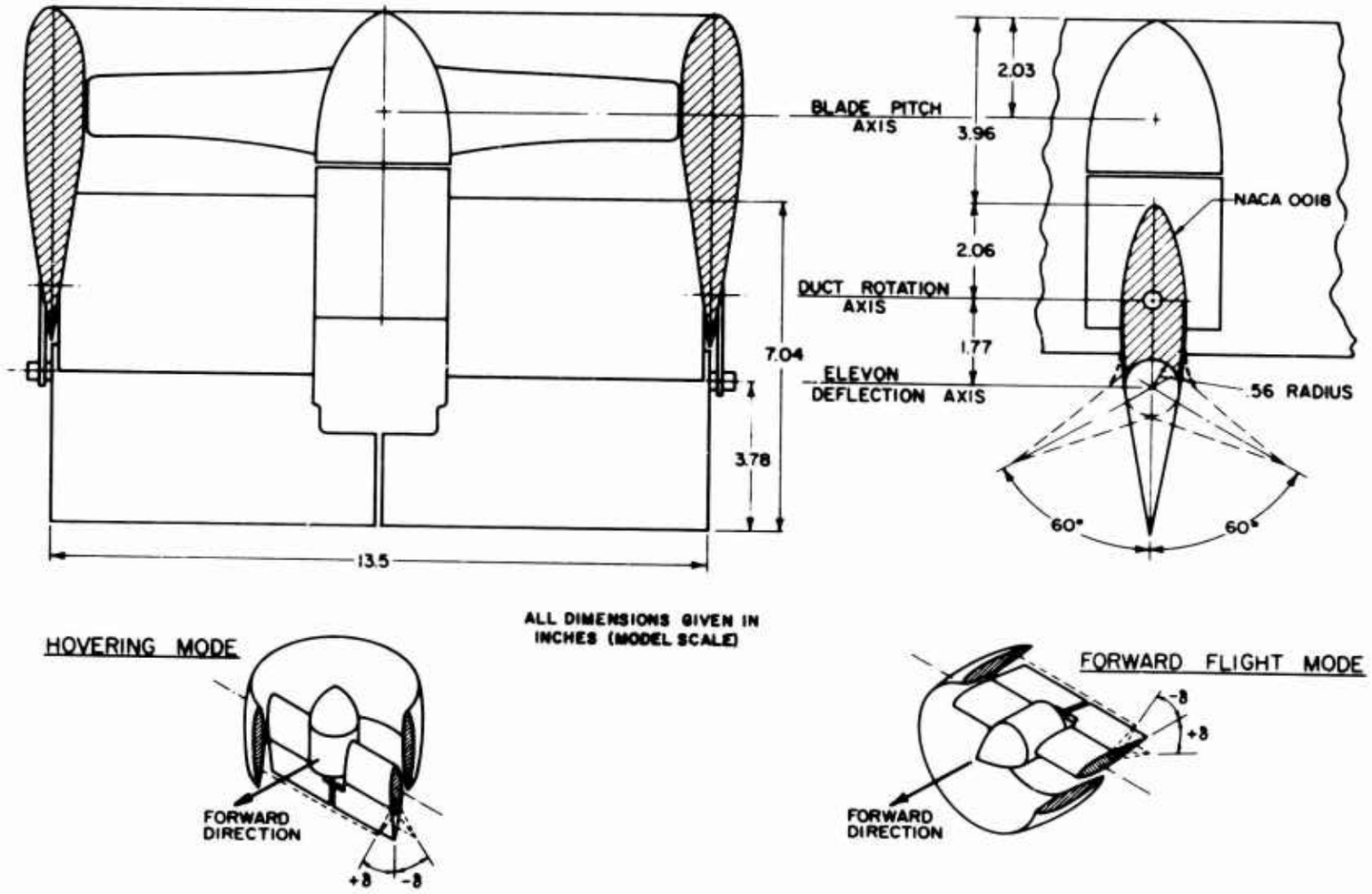

Figure 7. Geometric Characteristics and Reference Locations for Model Duct System.

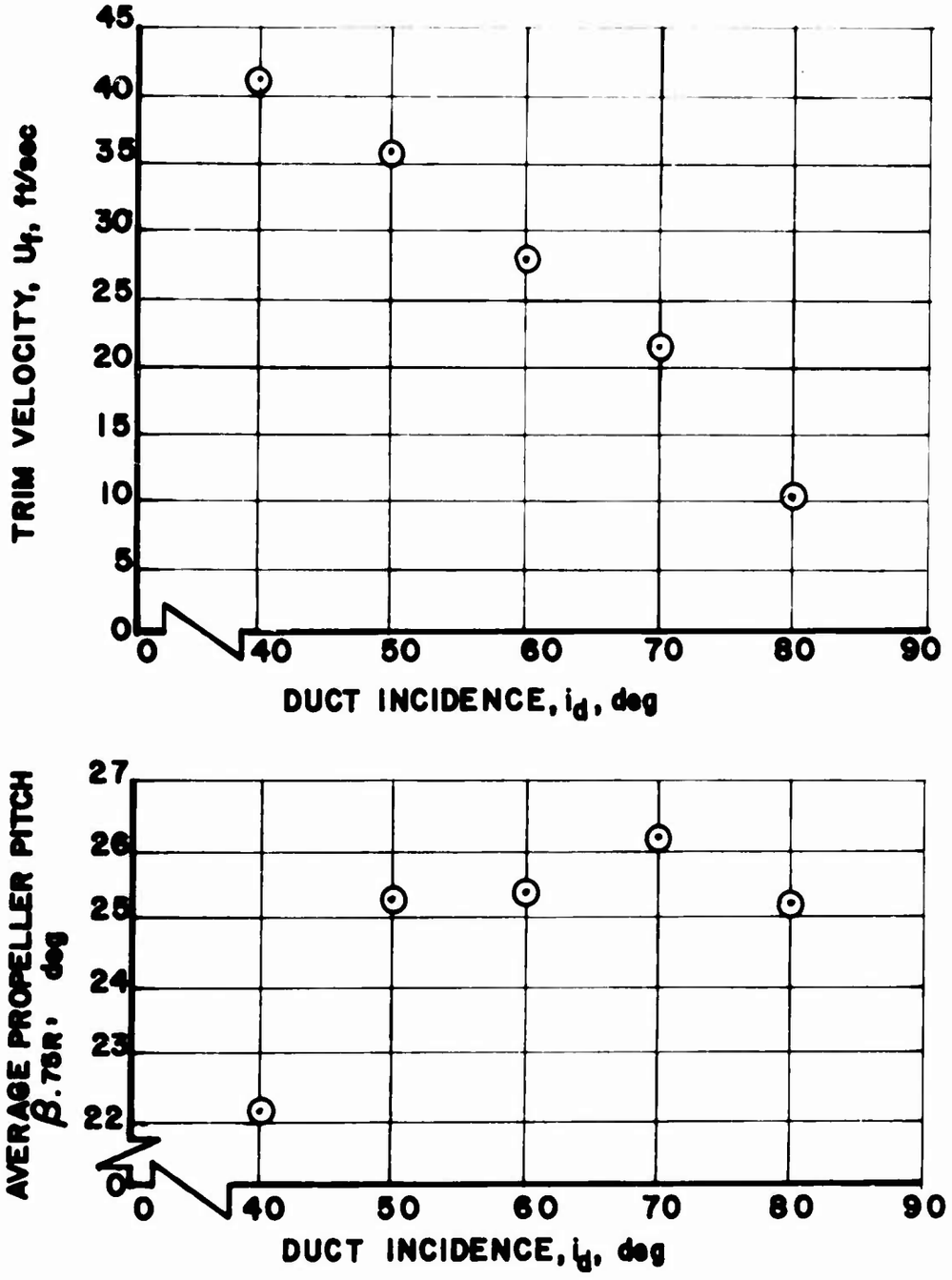

Figure 8. Experimental Data, Model Trim Conditions. Model Lift = Model Weight = 51.5 lb, rpm = 6780.

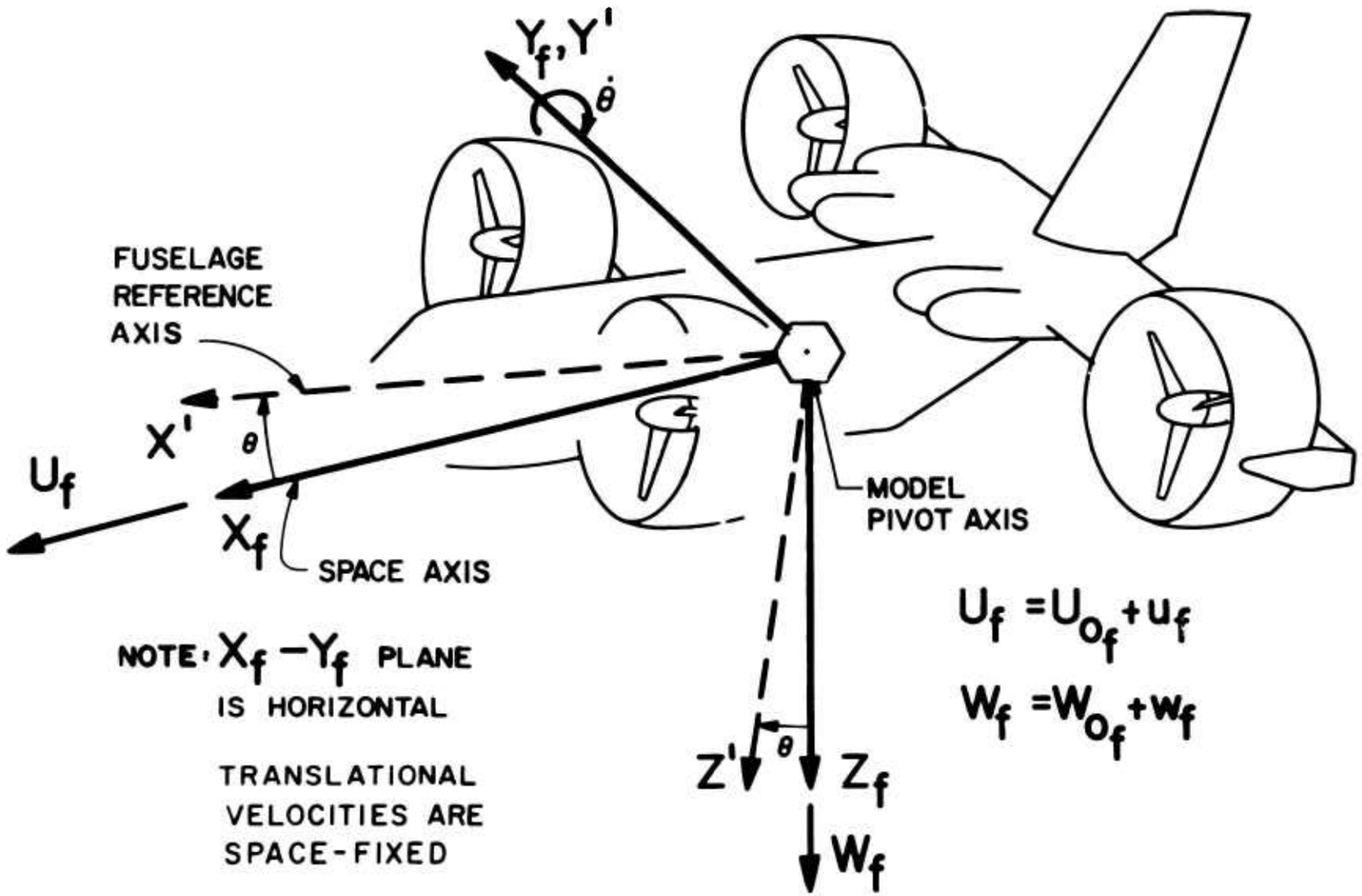

Figure 9. Axis System for Longitudinal Transient Response Data.

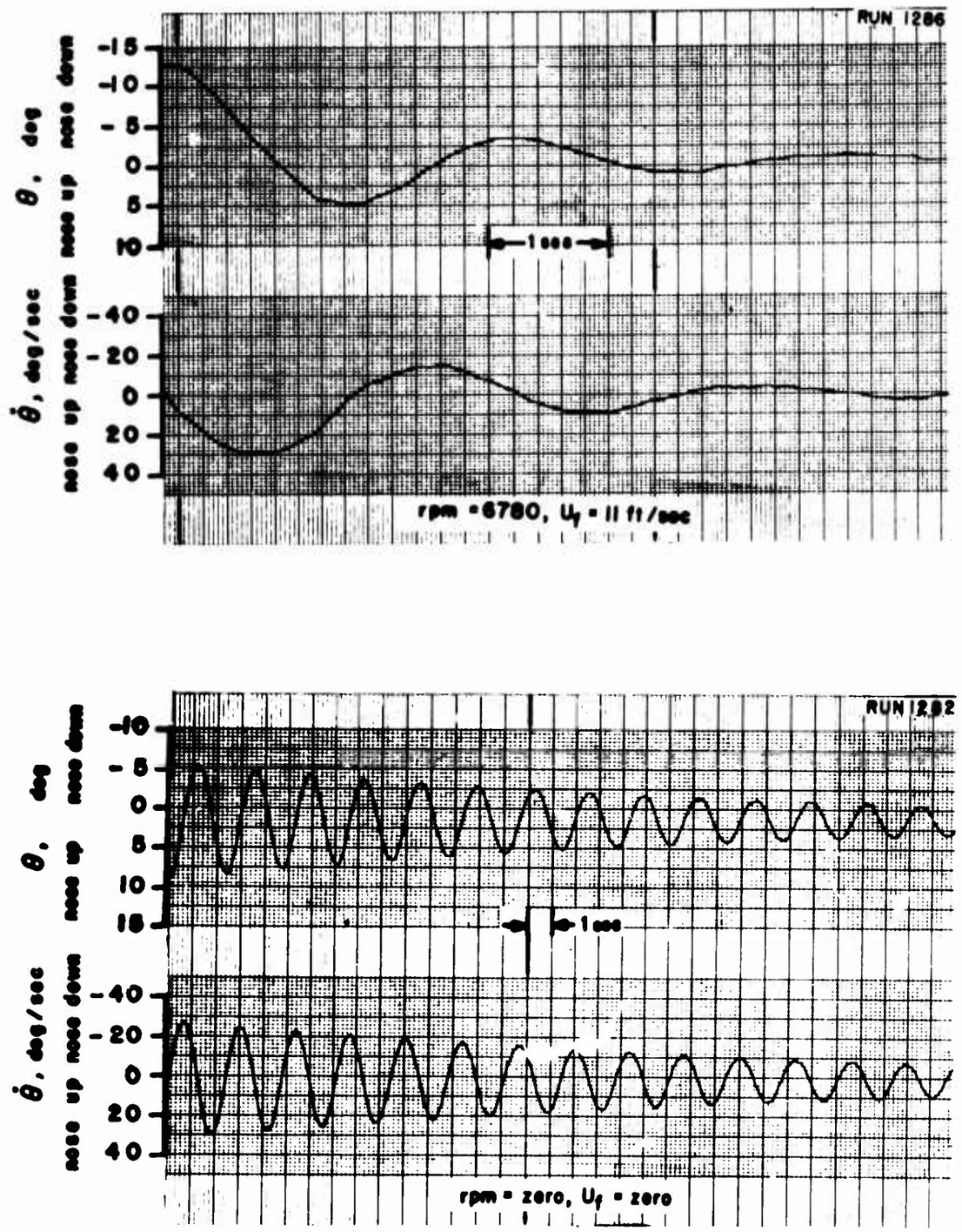

Figure 10. Self-Excited Transient Response. One Degree of Freedom, θ. No Stability Augmentation.
$i_d = 80°$, $\beta_{.75R} = 25.2°$.

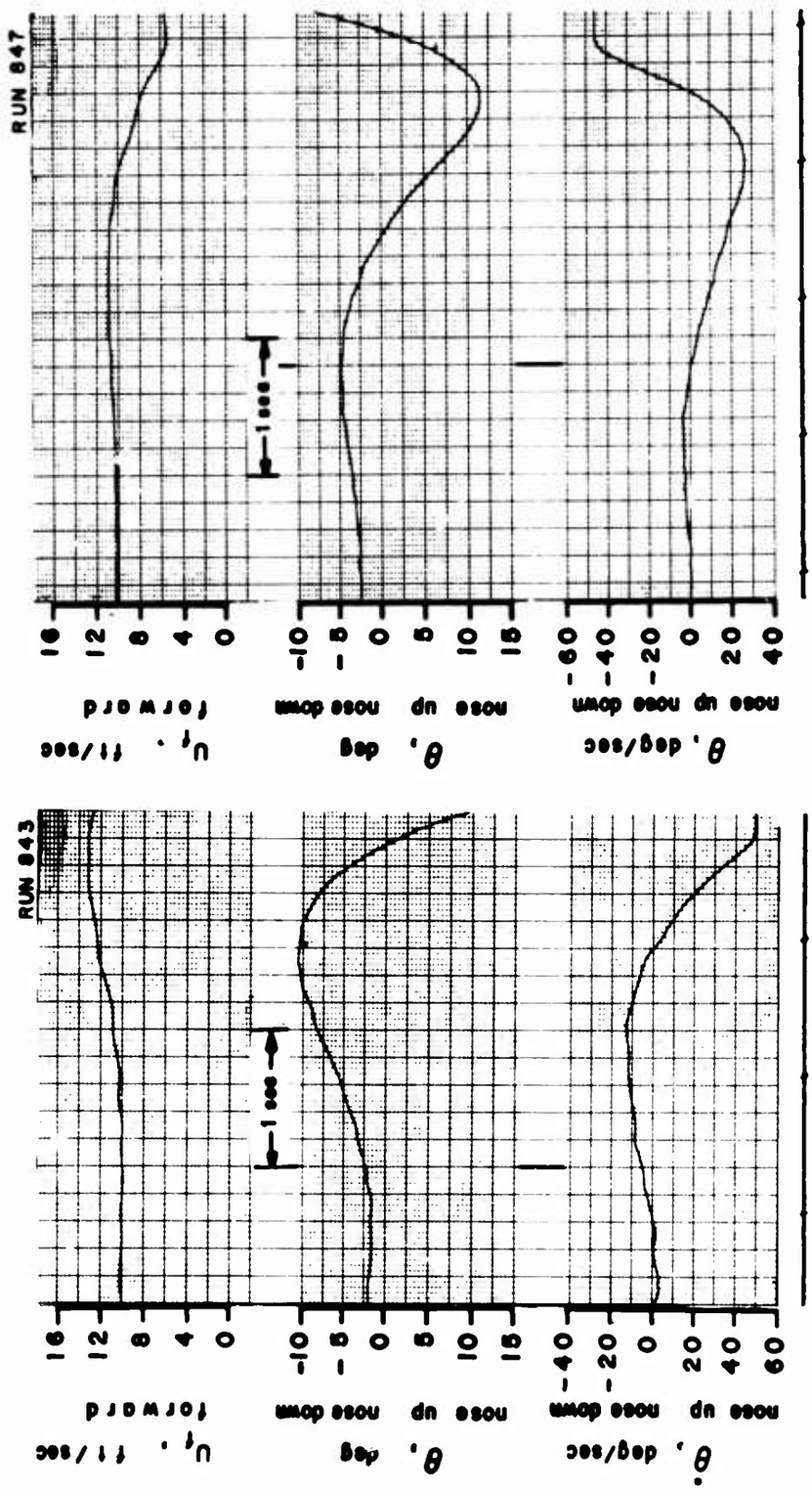

Figure 11. Self-Excited Transient Responses. Two Degrees of Freedom, θ-U_f. No Stability Augmentation.
i_d = 80°, $\beta_{.75R}$ = 25.2°, rpm = 6780.

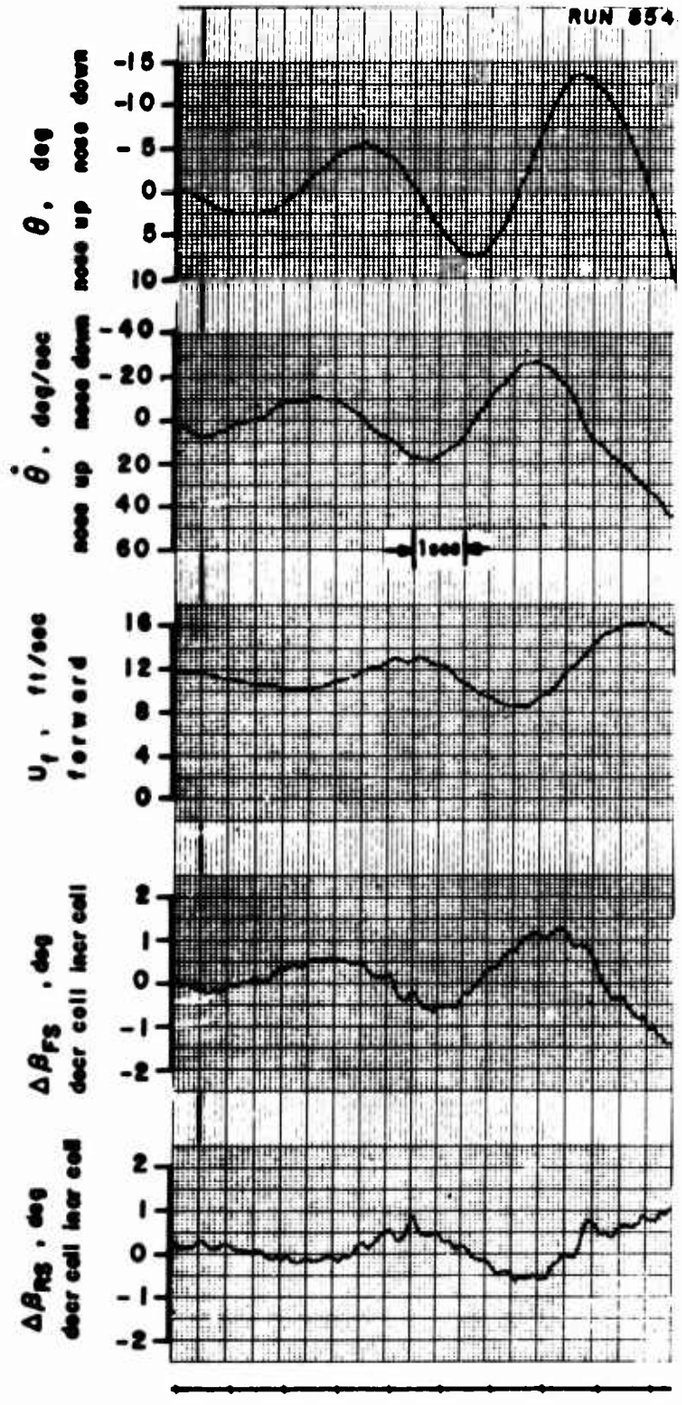

Figure 12. Self-Excited Transient Responses. Two Degrees of Freedom, θ-U_f. $K_{\dot{\theta}}$ = 0.030 sec.
i_d = 80°, $\beta_{.75R}$ = 25.2°, rpm = 6780.

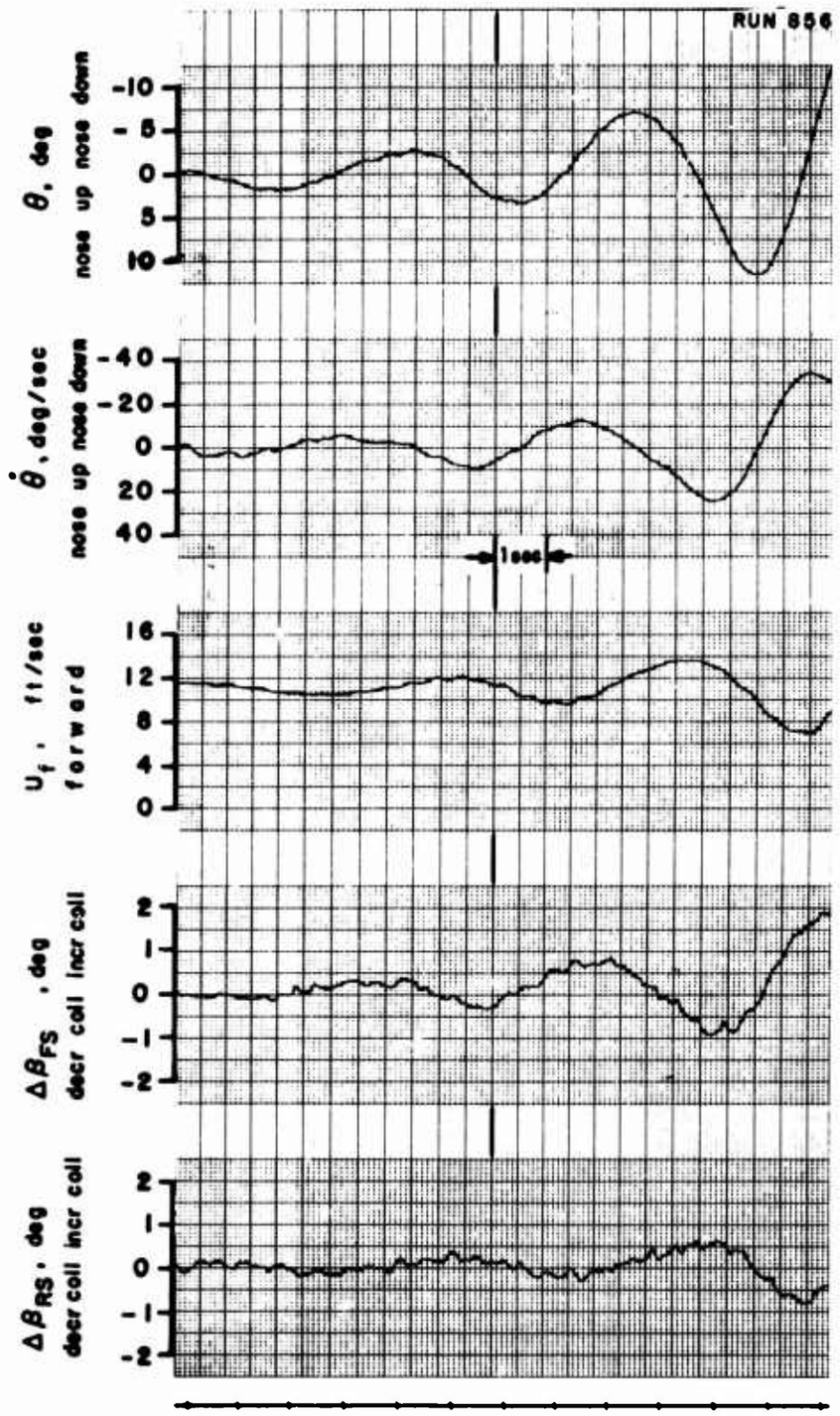

Figure 12. Concluded.

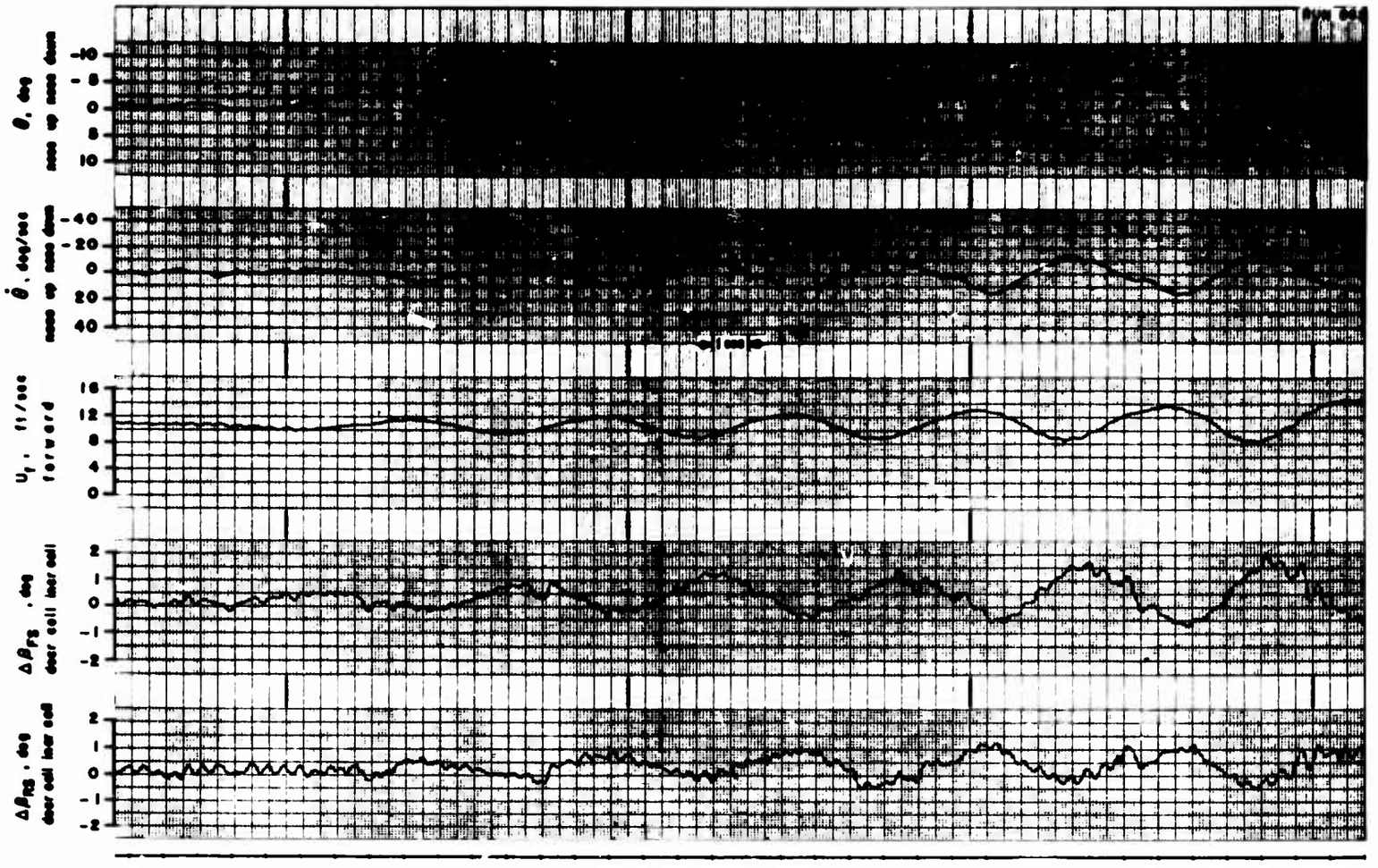

Figure 13. Self-Excited Transient Responses. Two Degrees of Freedom, θ-$\bar{U}_f$. $K_{\dot{\theta}}$ = 0.044 sec. i_d = 80°, $\beta_{.75R}$ = 25.2°, rpm = 6780.

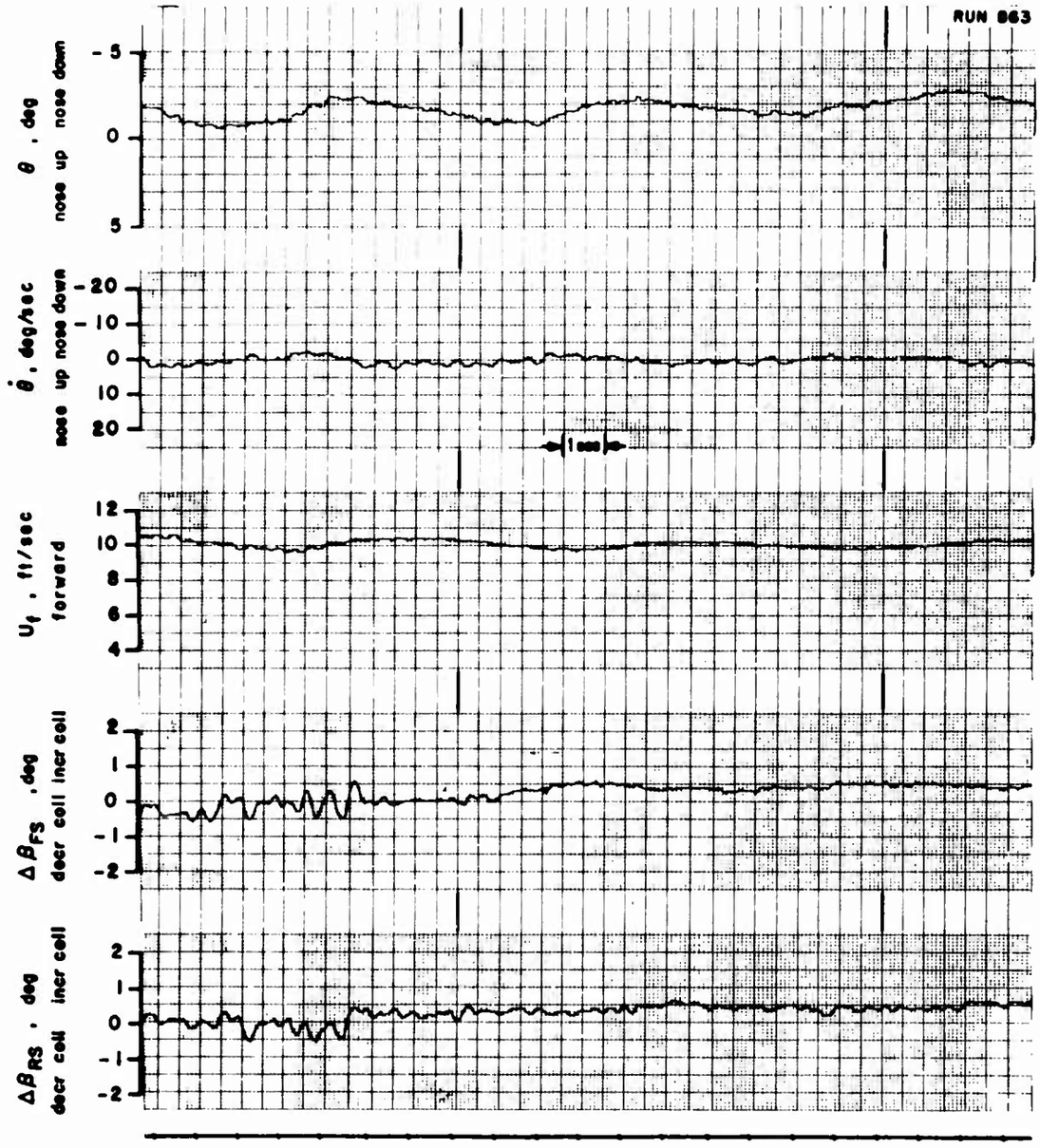

Figure 14. Self-Excited Transient Responses. Two Degrees of Freedom, θ-U_f. K°_{θ} = 0.060 sec.
i_d = 80°, $\beta_{.75R}$ = 25.2°, rpm = 6780.

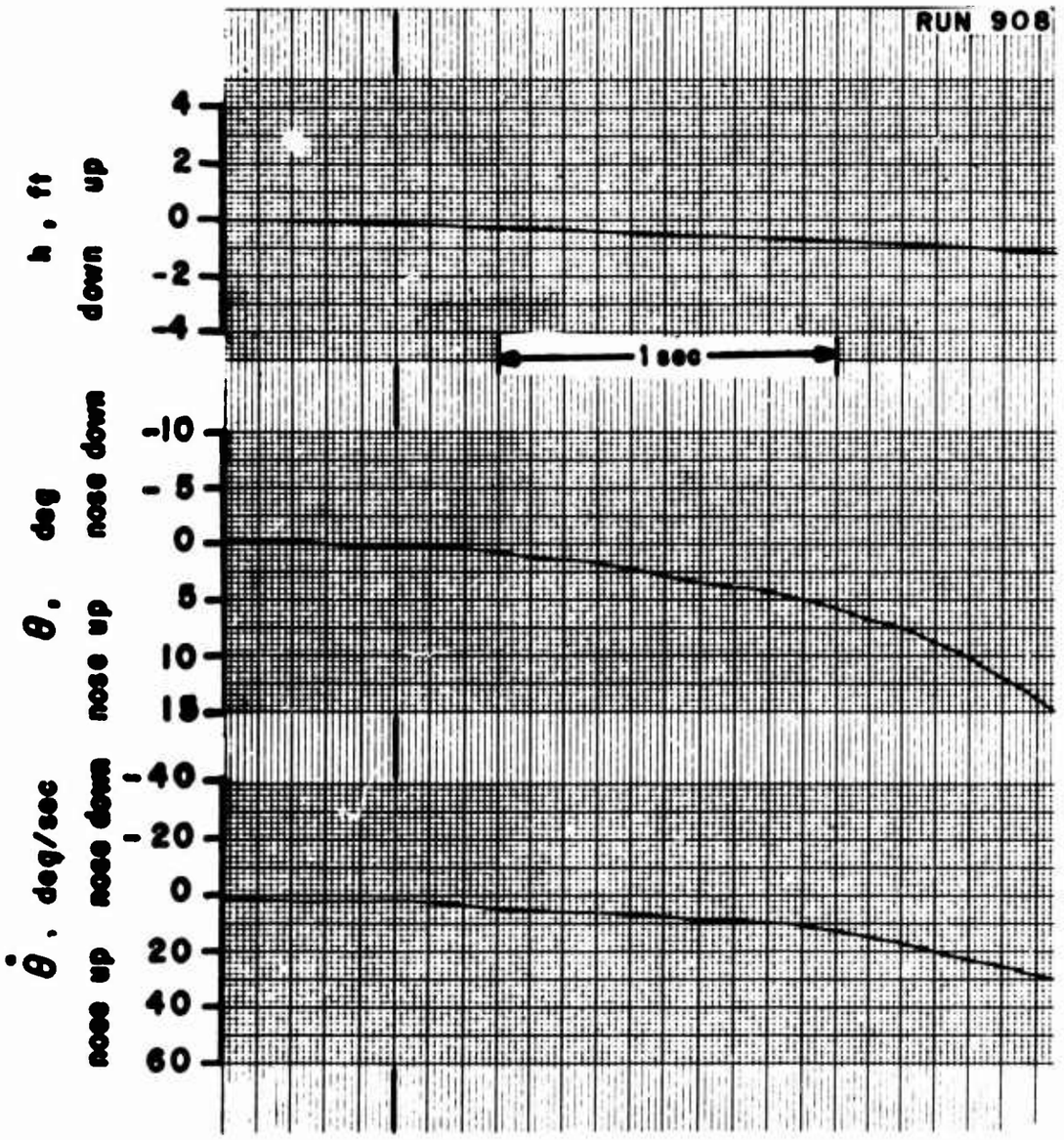

Figure 15. Self-Excited Transient Responses. Two Degrees of Freedom, θ-w_f. No Stability Augmentation.
$i_d = 80°$, $\beta_{.75R} = 23.7°$, rpm = 6780.

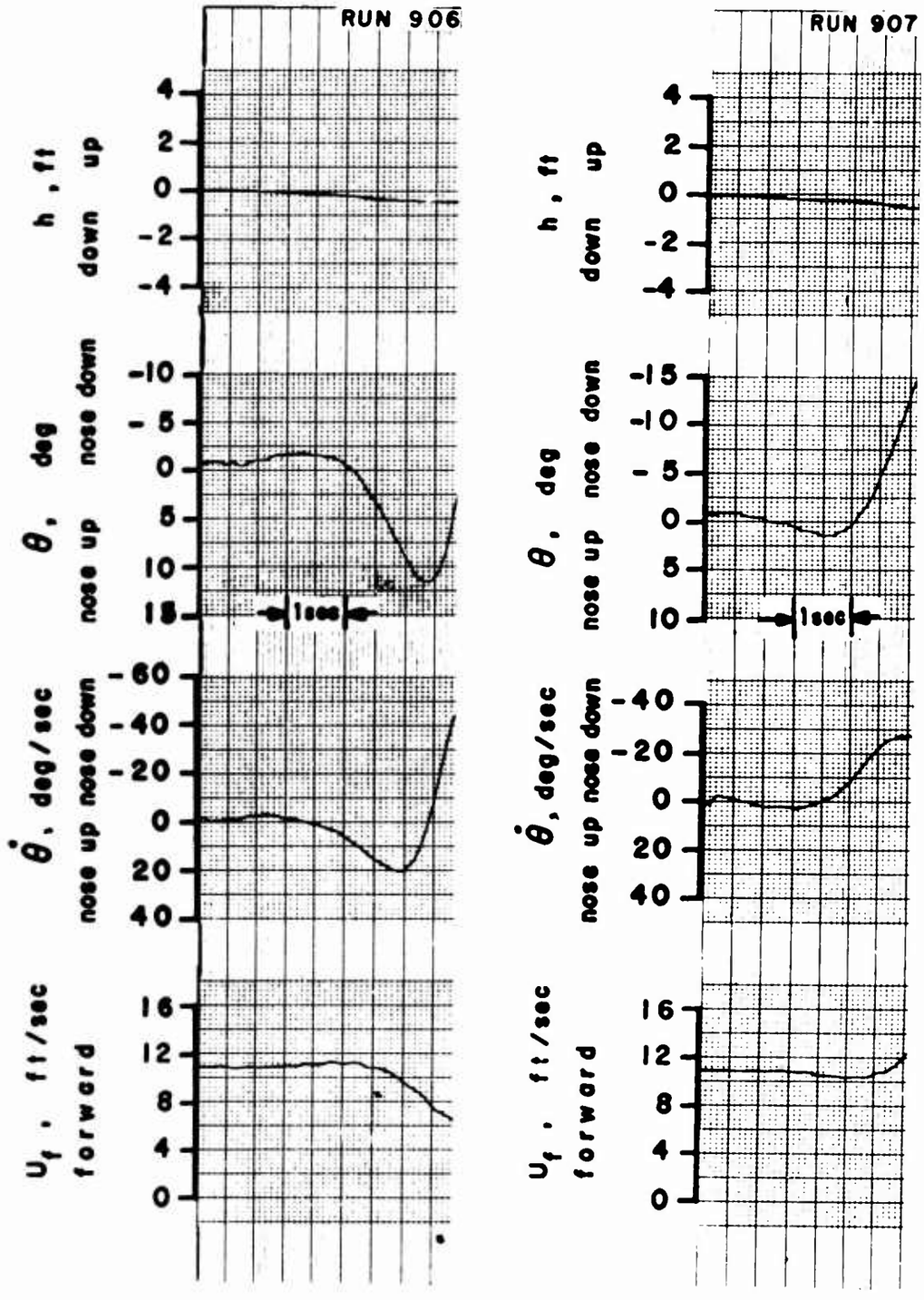

Figure 16. Self-Excited Transient Responses. Three Degrees of Freedom, θ-U_f-w_f. No Stability Augmentation.

i_d = 80°, $\beta_{.75R}$ = 23.7°, rpm = 6780.

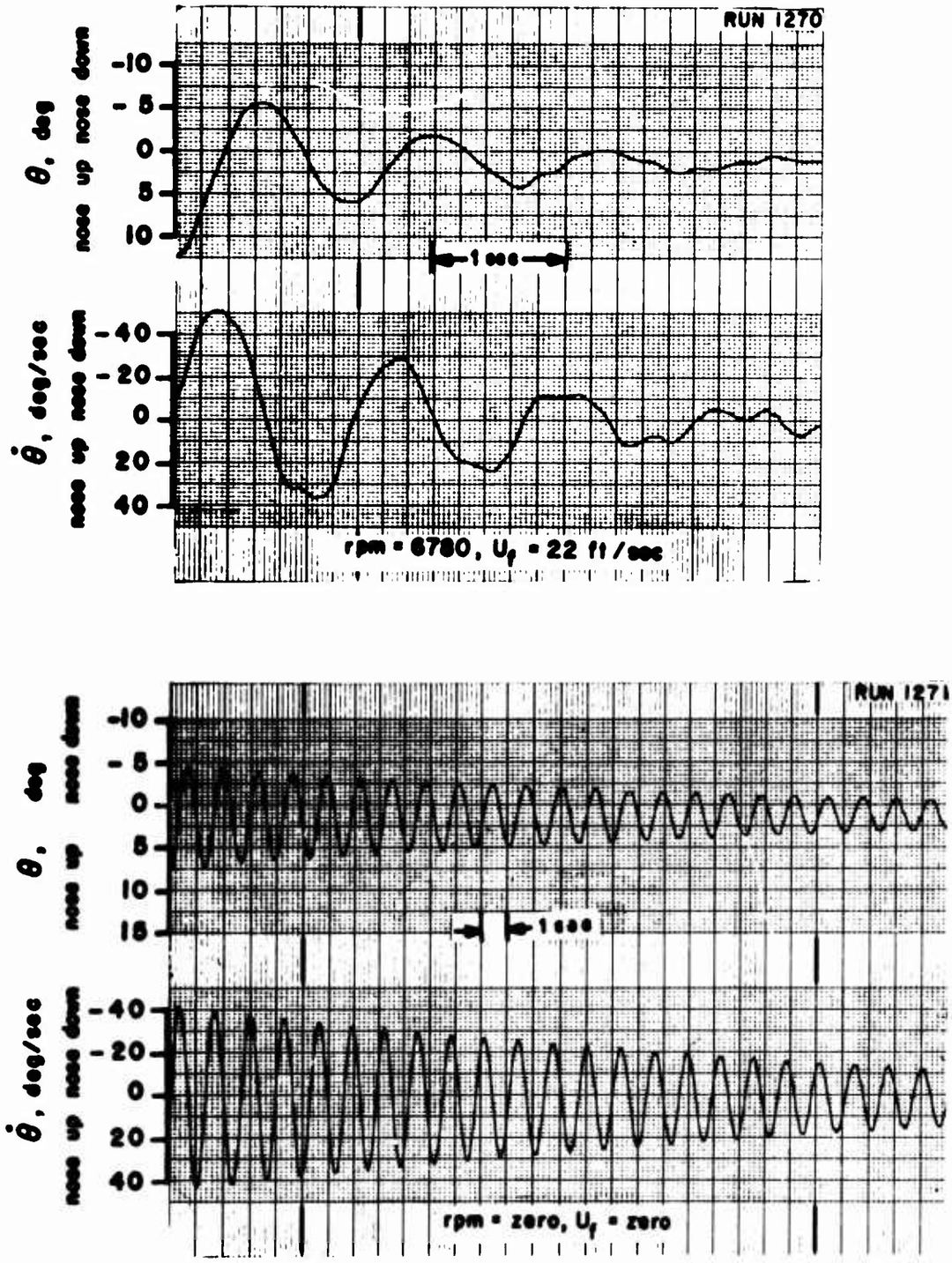

Figure 17. Self-Excited Transient Response. One Degree of Freedom, θ. No Stability Augmentation.
$i_d = 70°$, $\beta_{.75R} = 25.2°$.

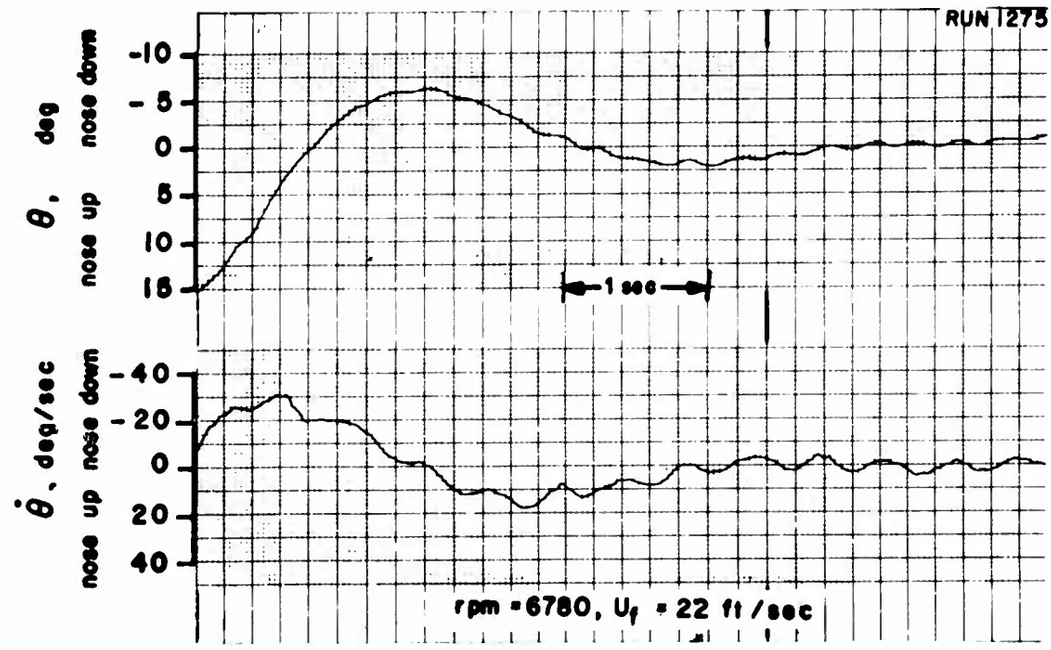

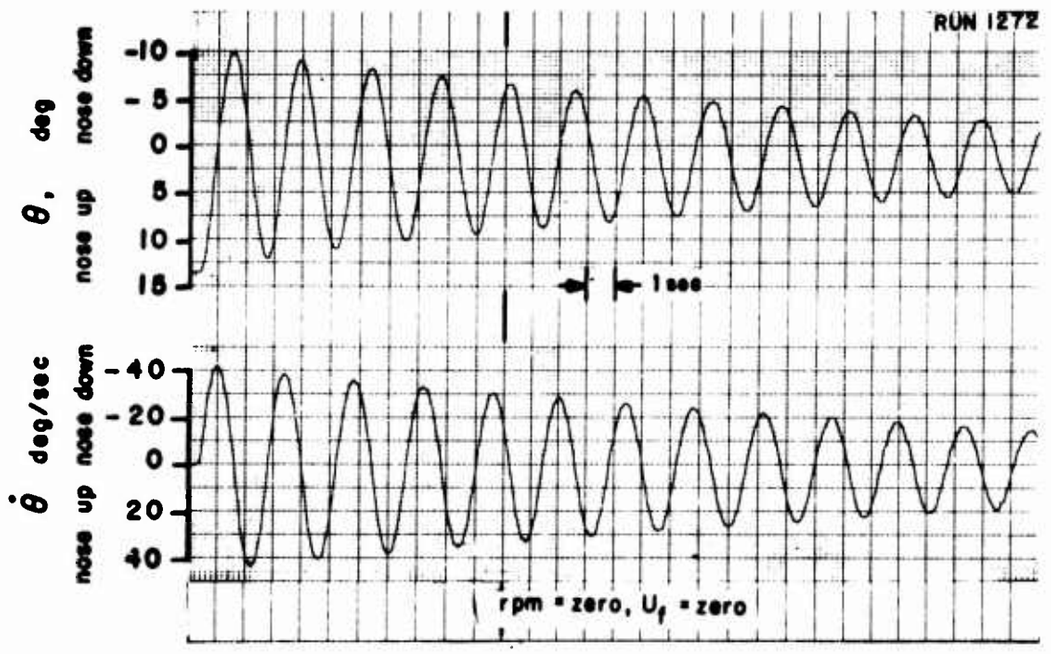

Figure 17. Concluded.

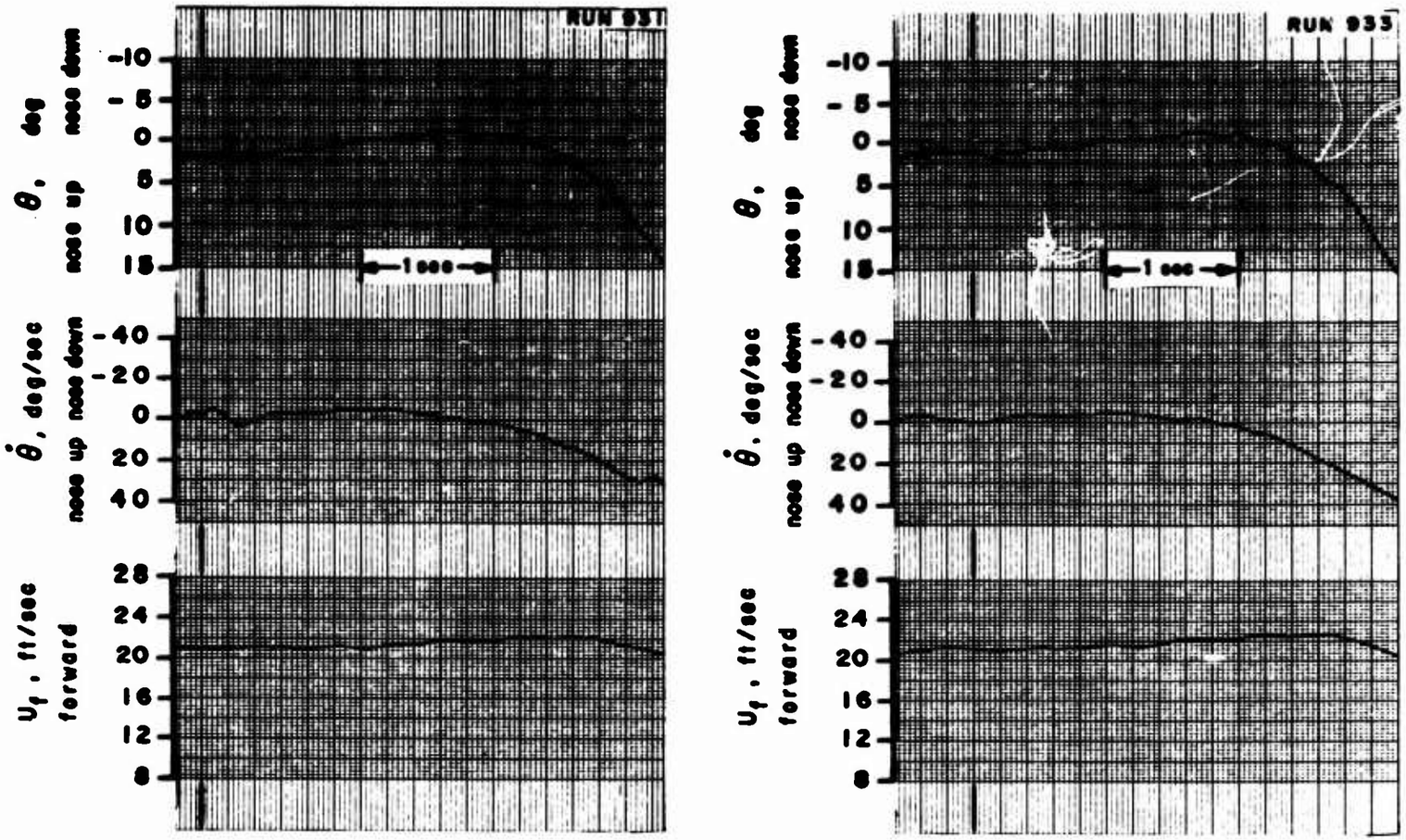

Figure 18. Self-Excited Transient Responses. Two Degrees of Freedom, θ-U_f. No Stability Augmentation.
$i_d = 70°$, $\beta_{.75R} = 26.2°$, rpm = 6780.

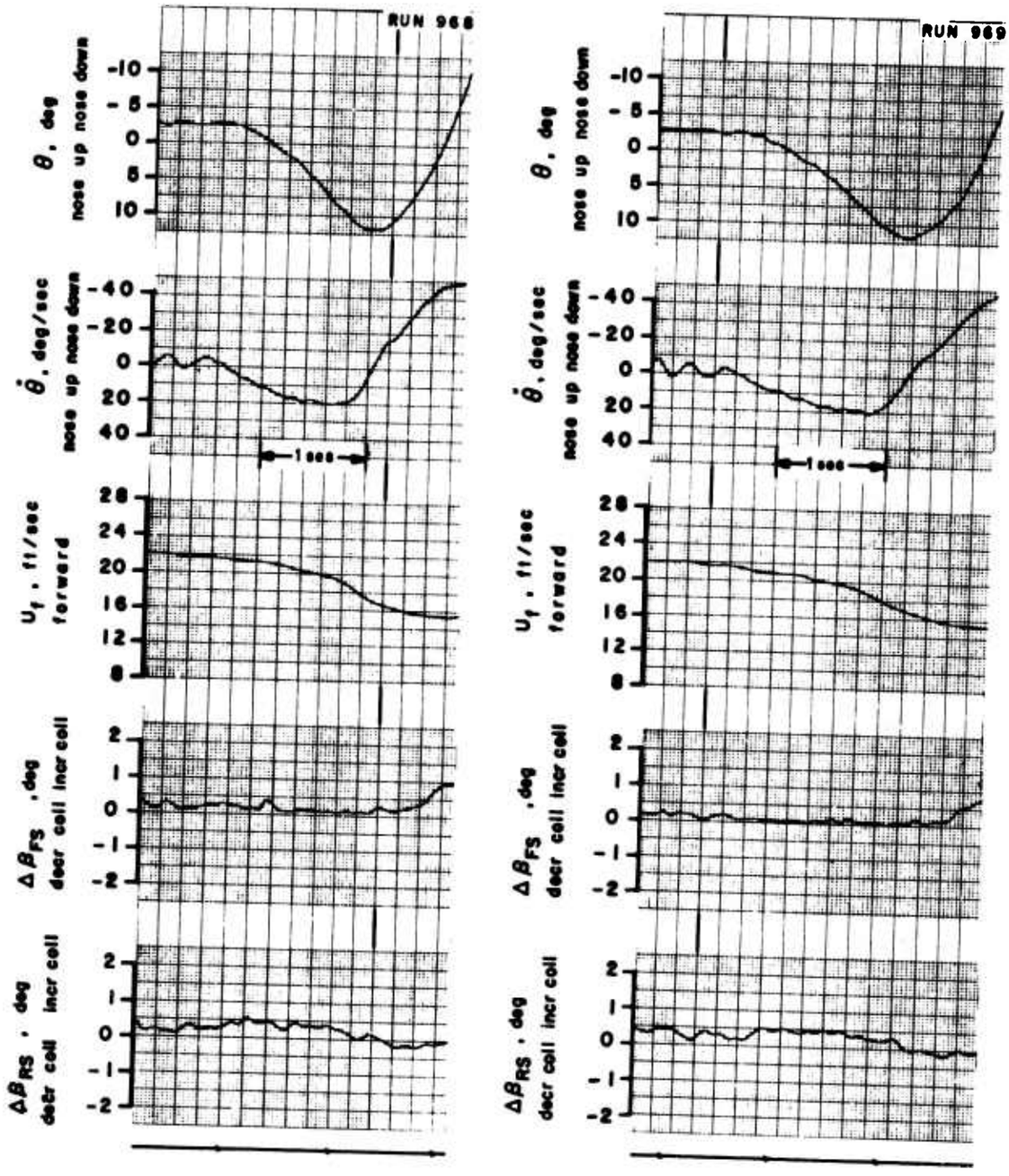

Figure 19. Self-Excited Transient Responses. Two Degrees of Freedom, θ-U_f. $K_{\dot{\theta}}$ = 0.021 sec.

i_d = 70°, $\beta_{.75R}$ = 26.2°, rpm = 6780.

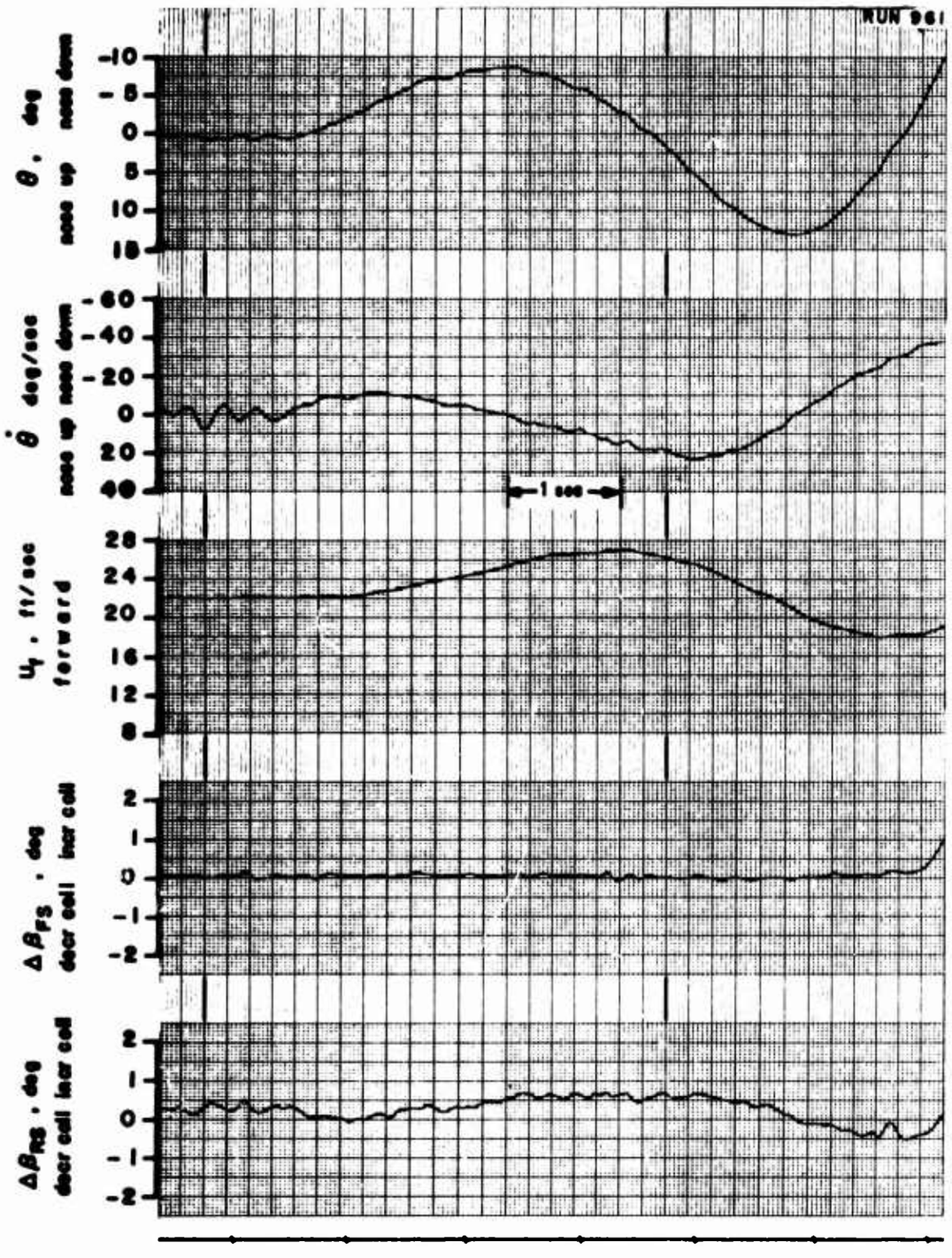

Figure 20. Self-Excited Transient Responses. Two Degrees of Freedom, θ-U_f. K_θ = 0.027 sec.
i_d = 70°, $\beta_{.75R}$ = 26.2°, rpm = 6780.

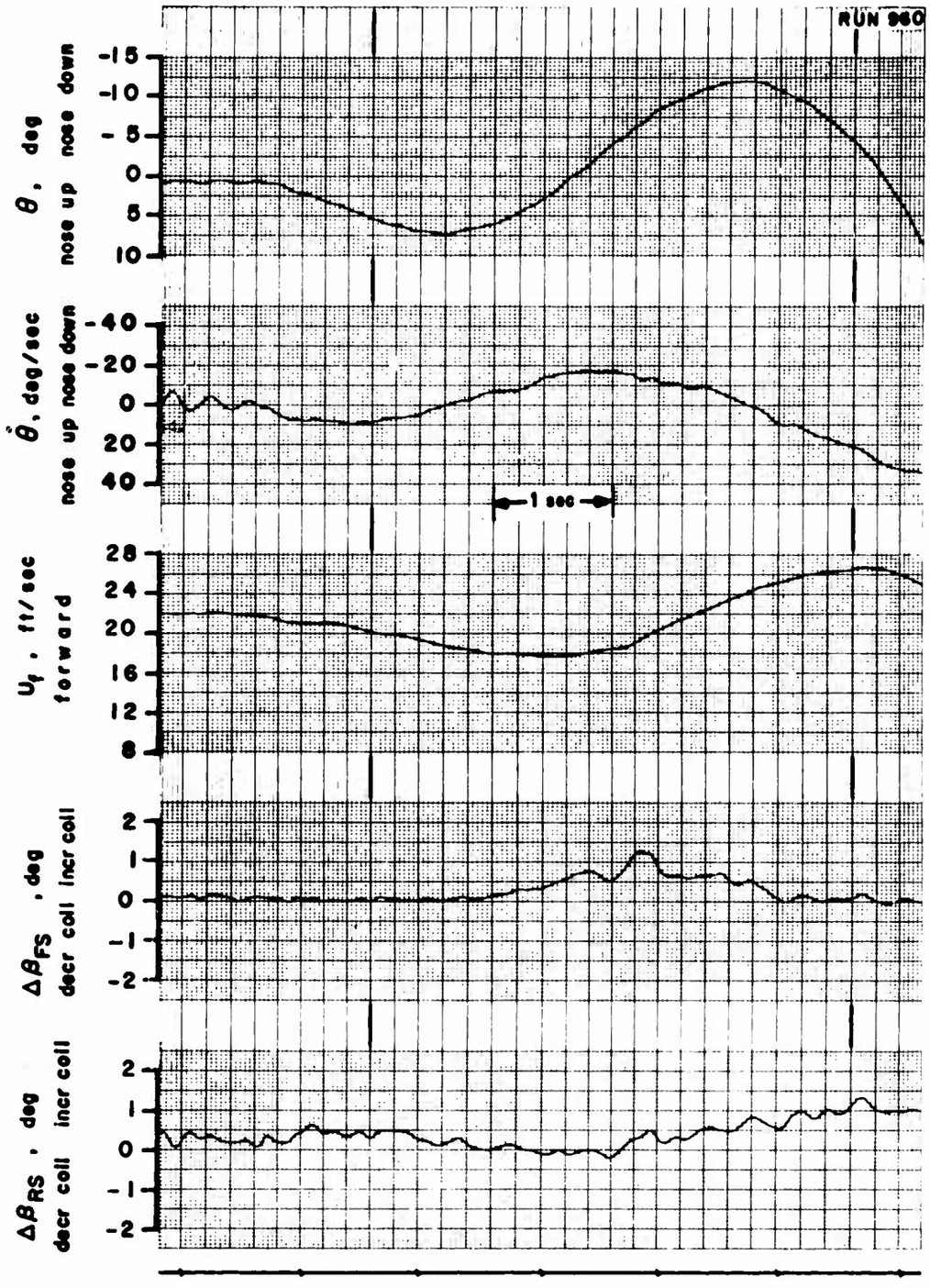

Figure 21. Self-Excited Transient Responses. Two Degrees of Freedom, θ-U_f. $K_{\dot{\theta}}$ = 0.030 sec.
i_d = 70°, $\beta_{.75R}$ = 26.2°, rpm = 6780.

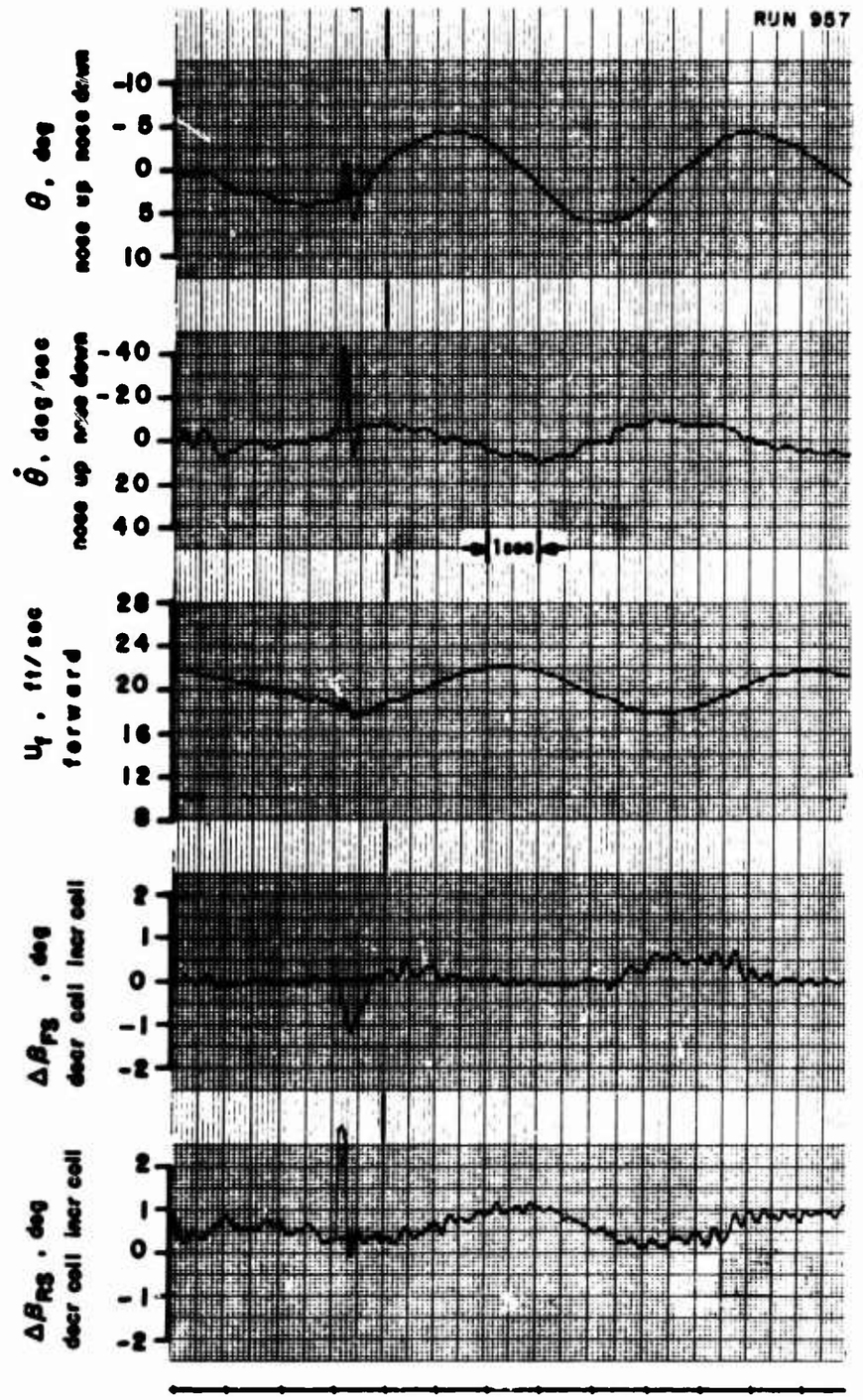

Figure 22. Self-Excited Transient Responses. Two Degrees of Freedom, θ-U_f. $K_{\dot{\theta}}^{s}$ = 0.044 sec.
i_d = 70°, $\beta_{.75R}$ = 26.2°, rpm = 6780.

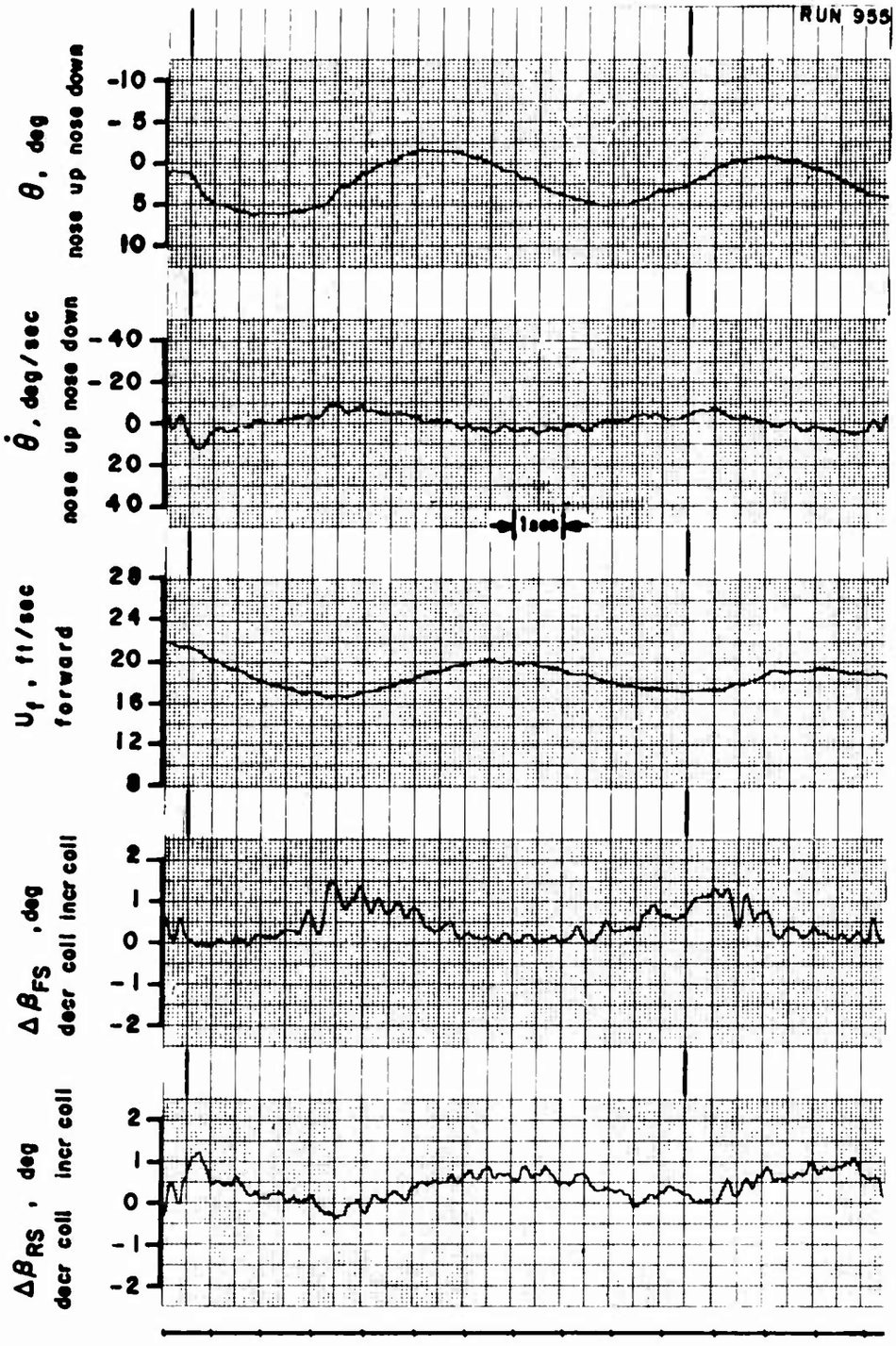

Figure 23. Self-Excited Transient Responses. Two Degrees of Freedom, θ-U_f. $K_{\dot{\theta}}$ = 0.060 sec.

i_d = 70°, $\beta_{.75R}$ = 26.2°, rpm = 6780.

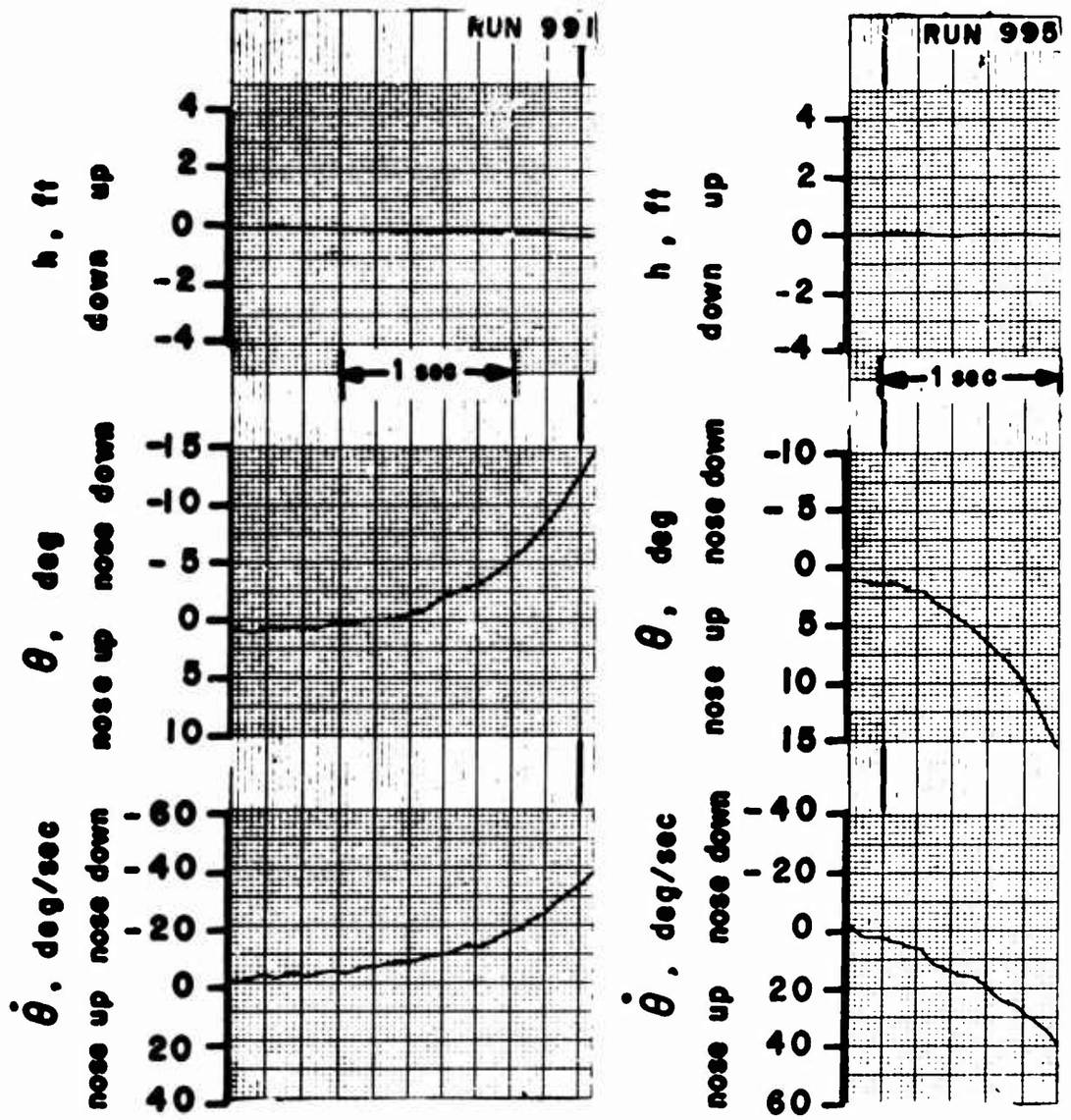

Figure 24. Self-Excited Transient Responses. Two Degrees of Freedom, θ-w_f. No Stability Augmentation.
$i_d = 70°$, $\beta_{.75R} = 26.2°$, rpm = 6780.

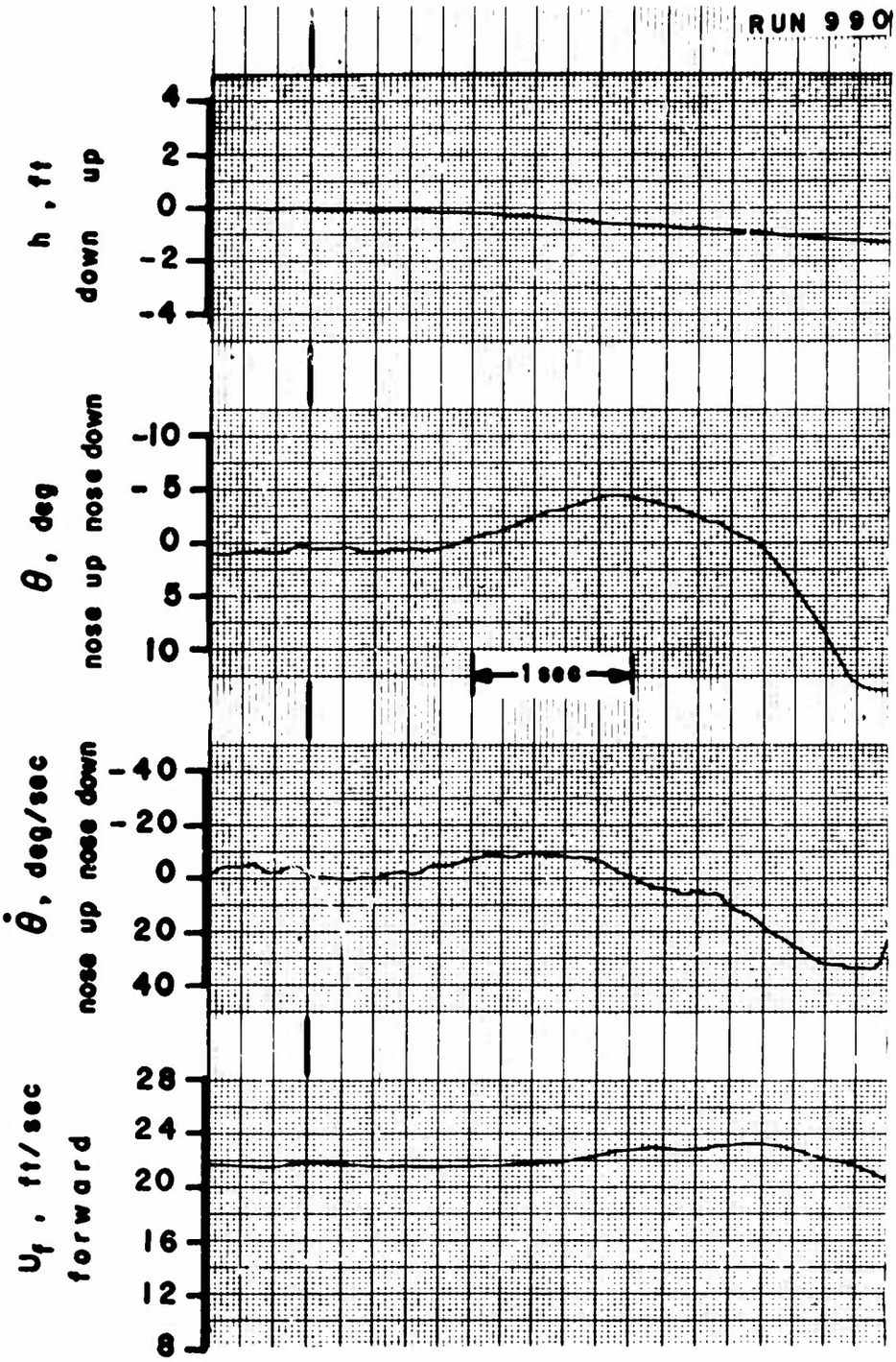

Figure 25. Self-Excited Transient Responses. Three Degrees of Freedom, θ-U_f-w_f. No Stability Augmentation.
i_d = 70°, $\beta_{.75R}$ = 26.2°, rpm = 6780.

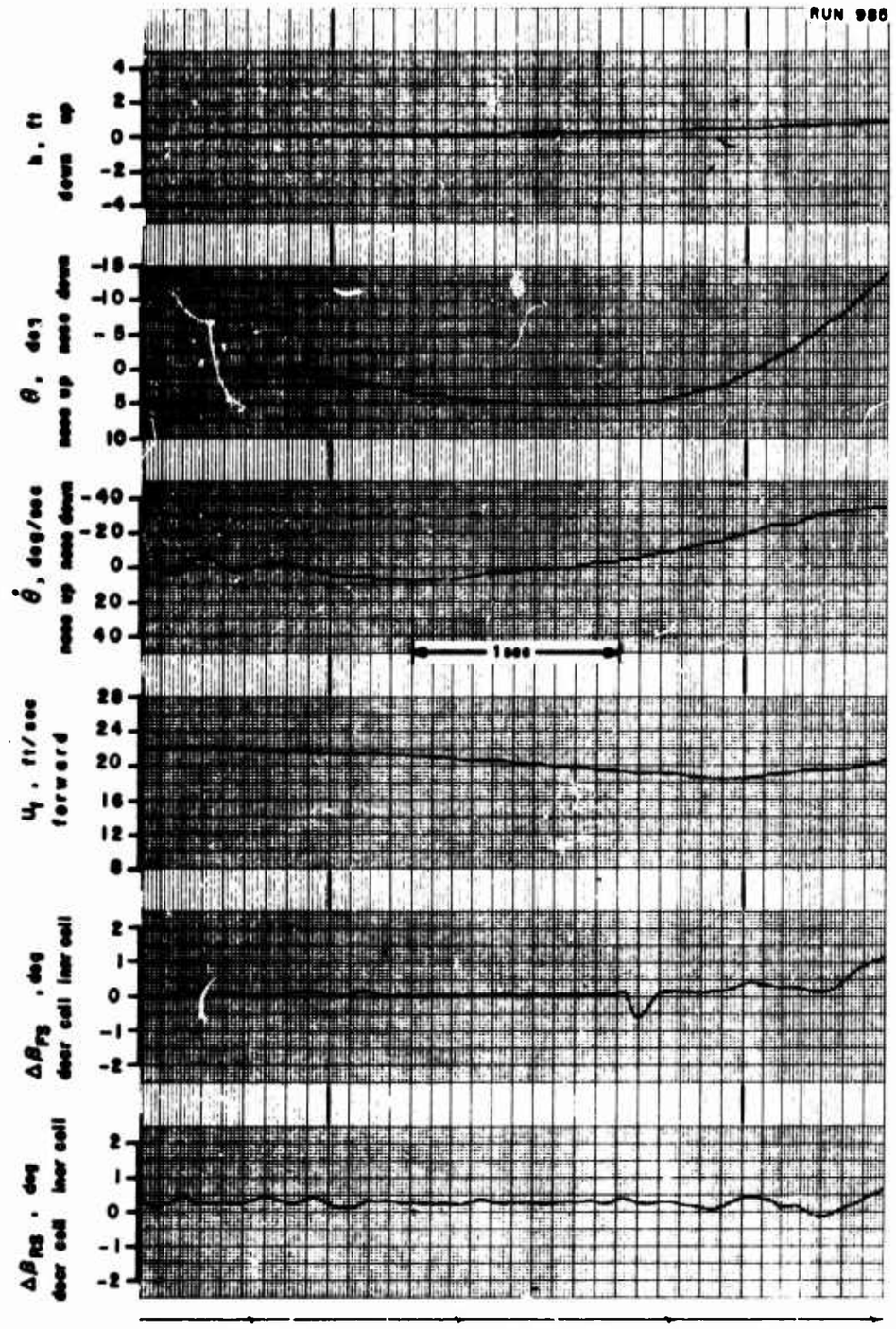

Figure 26. Self-Excited Transient Responses. Three Degrees of Freedom, θ-U_f-w_f. $K_{\dot{\theta}}$ = 0.021 sec.

i_d = 70°, $\beta_{.75R}$ = 26.2°, rpm = 6780.

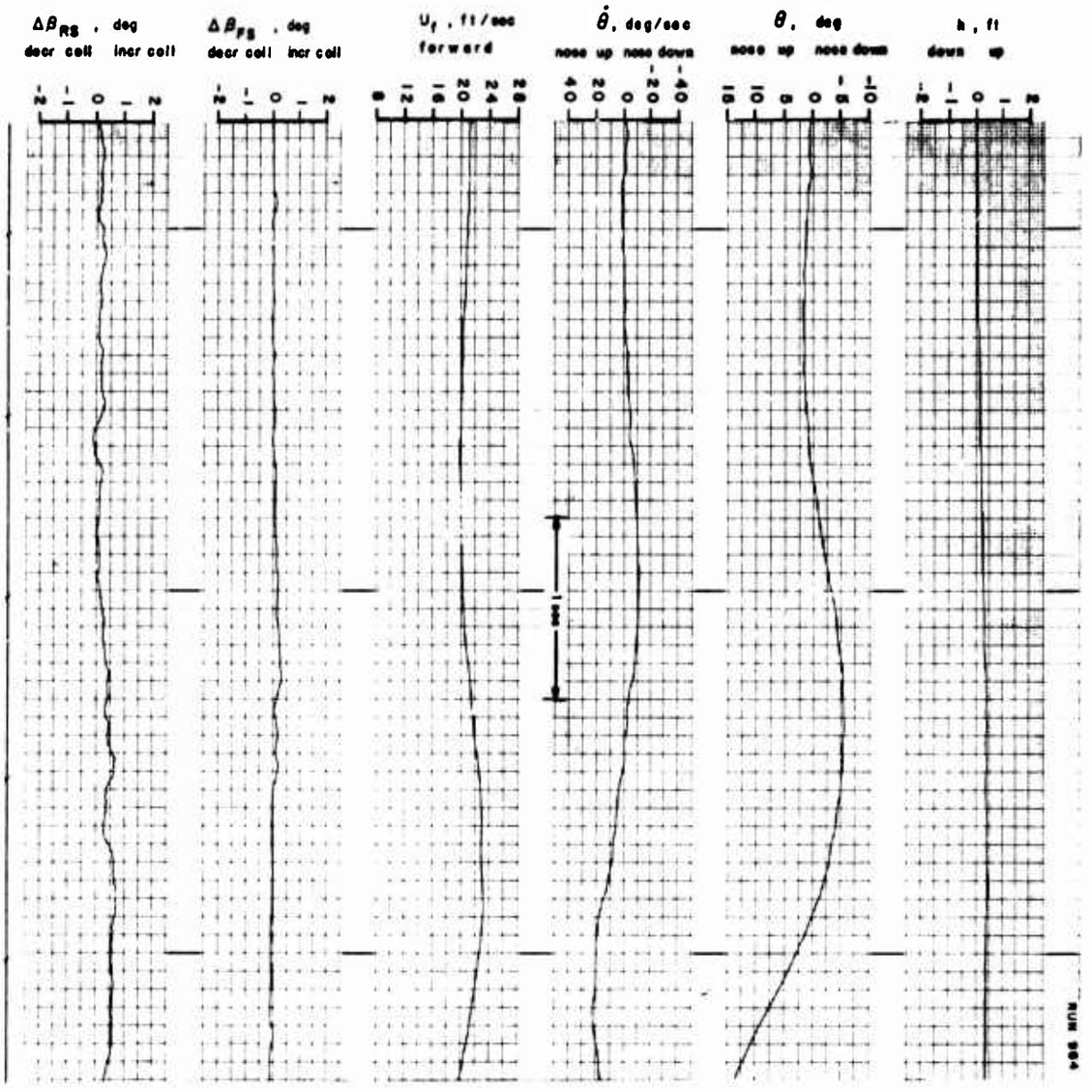

Figure 27. Self-Excited Transient Responses. Three Degrees of Freedom, θ-U_f-w_f. $K_{\dot{\theta}}$ = 0.027 sec.

i_d = 70°, $\beta_{.75R}$ = 26.2°, rpm = 6780.

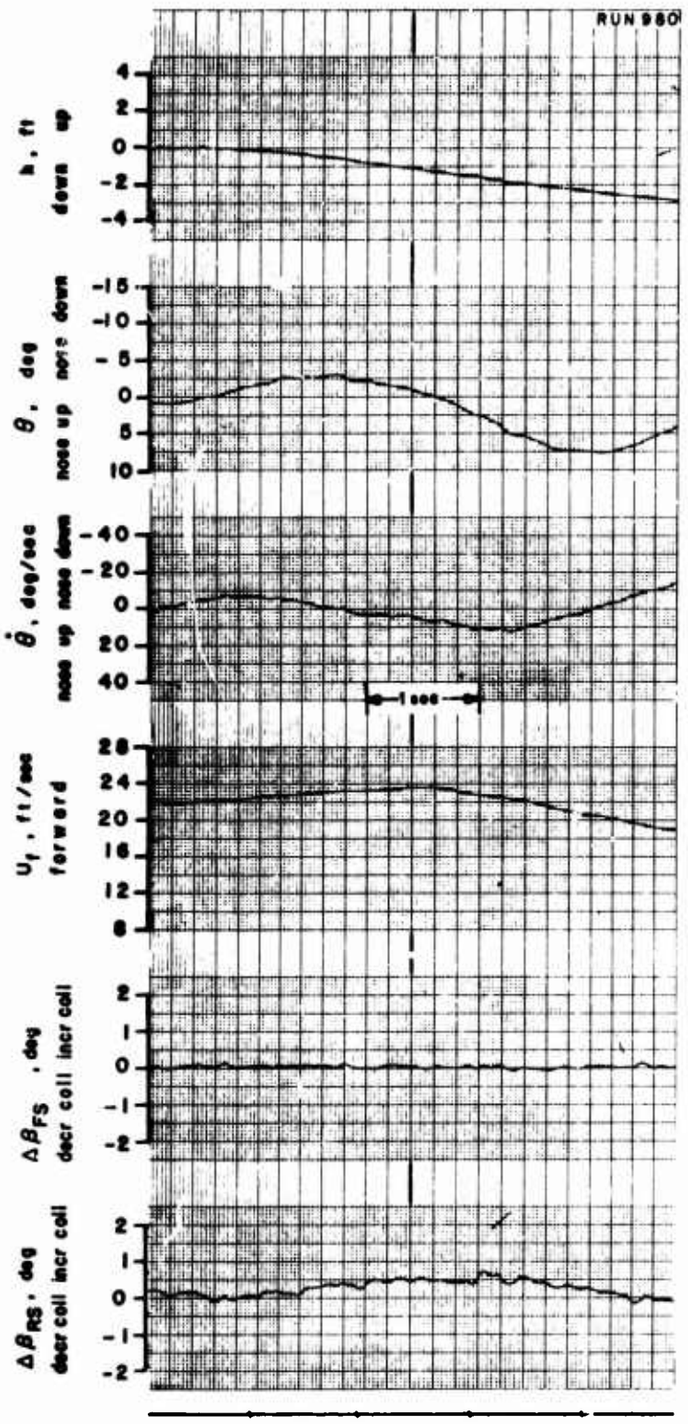

Figure 28. Self-Excited Transient Responses. Three Degrees of Freedom, θ-U_f-w_f. $K_{\dot{\theta}}$ = 0.030 sec.
i_d = 70°, $\beta_{.75R}$ = 26.2°, rpm = 6780.

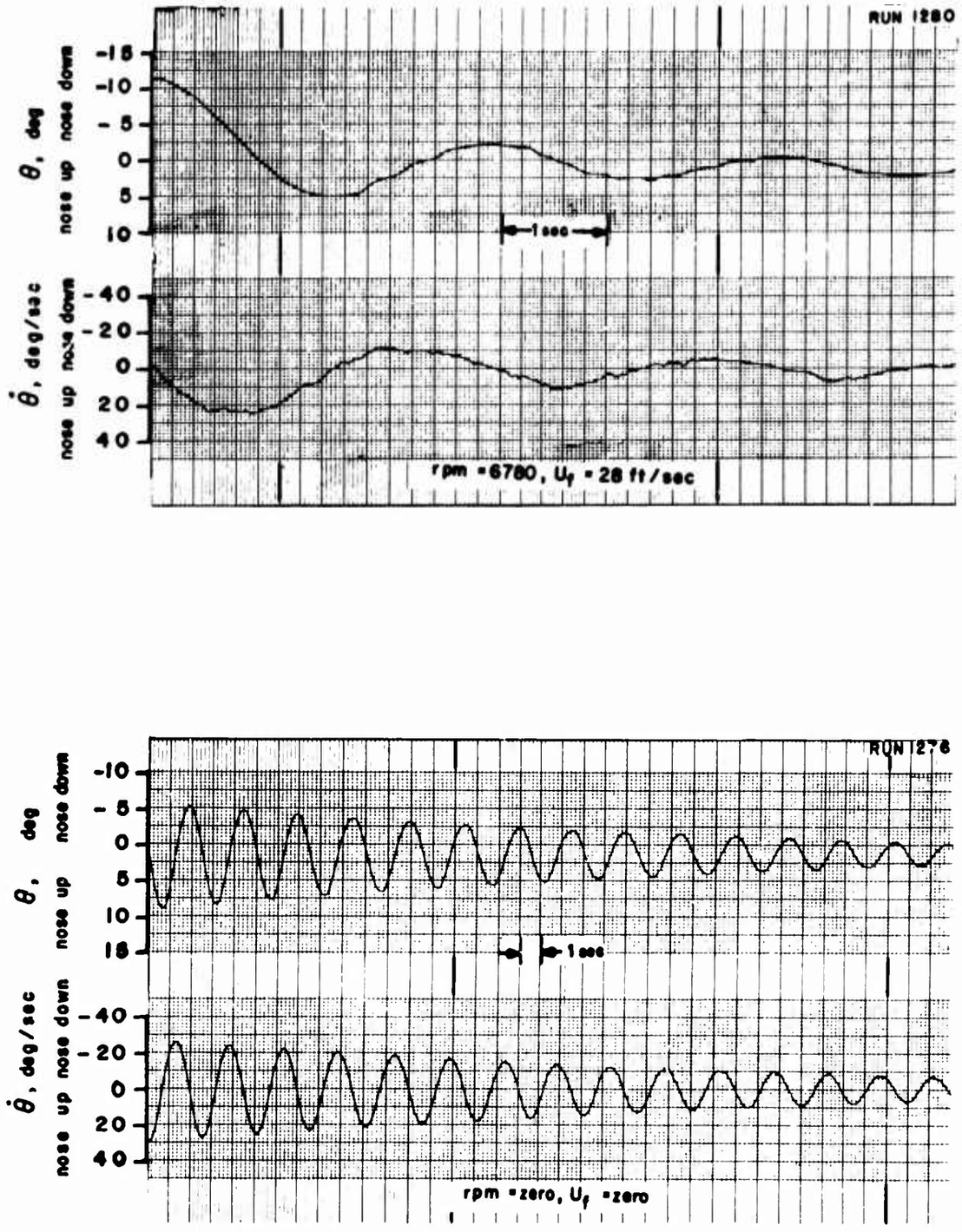

Figure 29. Self-Excited Transient Response. One Degree of Freedom, θ. No Stability Augmentation.
$i_d = 60°$, $\beta_{.75R} = 25.5°$.

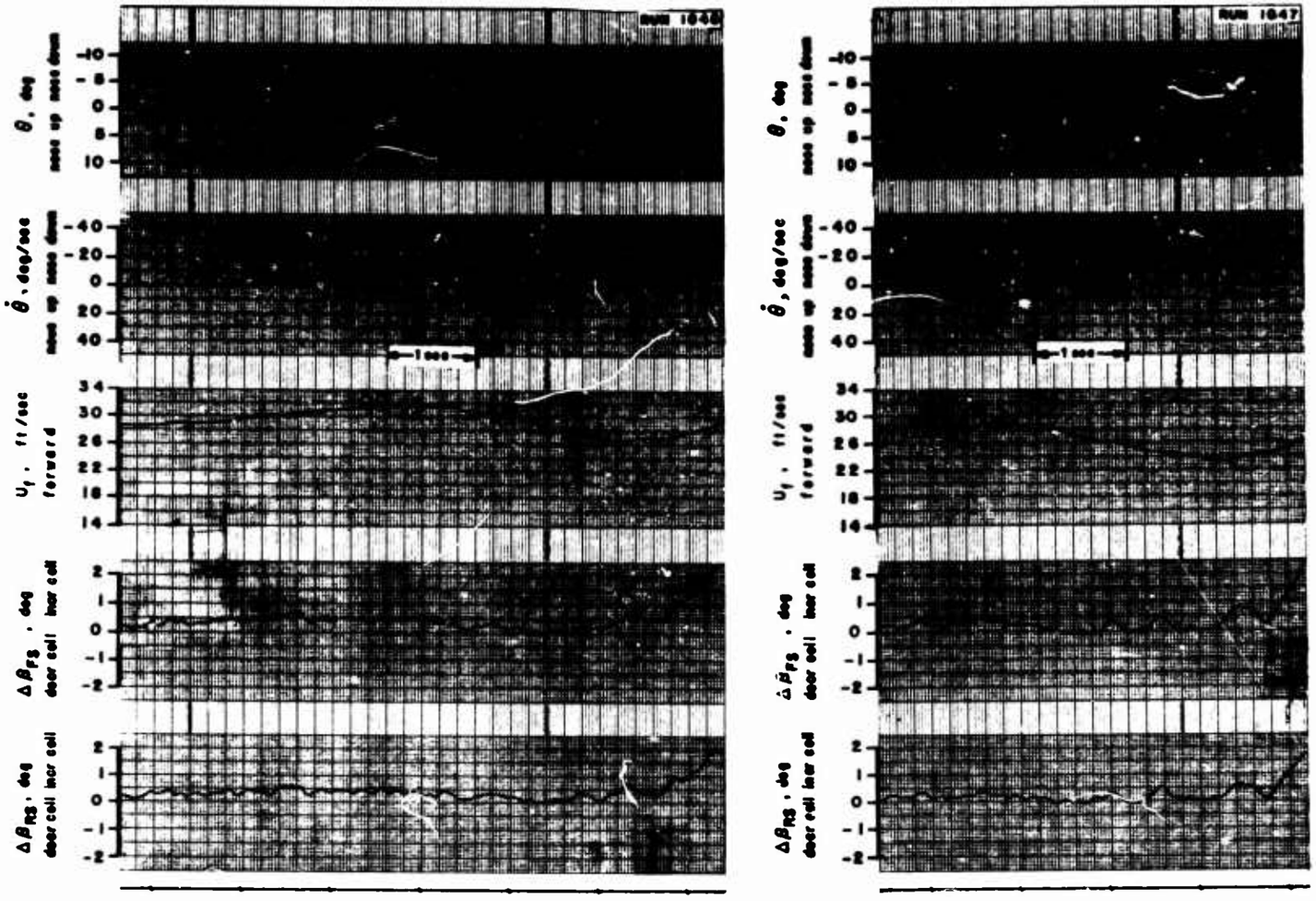

Figure 30. Self-Excited Transient Responses. Two Degrees of Freedom, θ-U_f. No Stability Augmentation.
$i_d = 60°$, $\beta_{.75R} = 25.4°$, rpm = 6780.

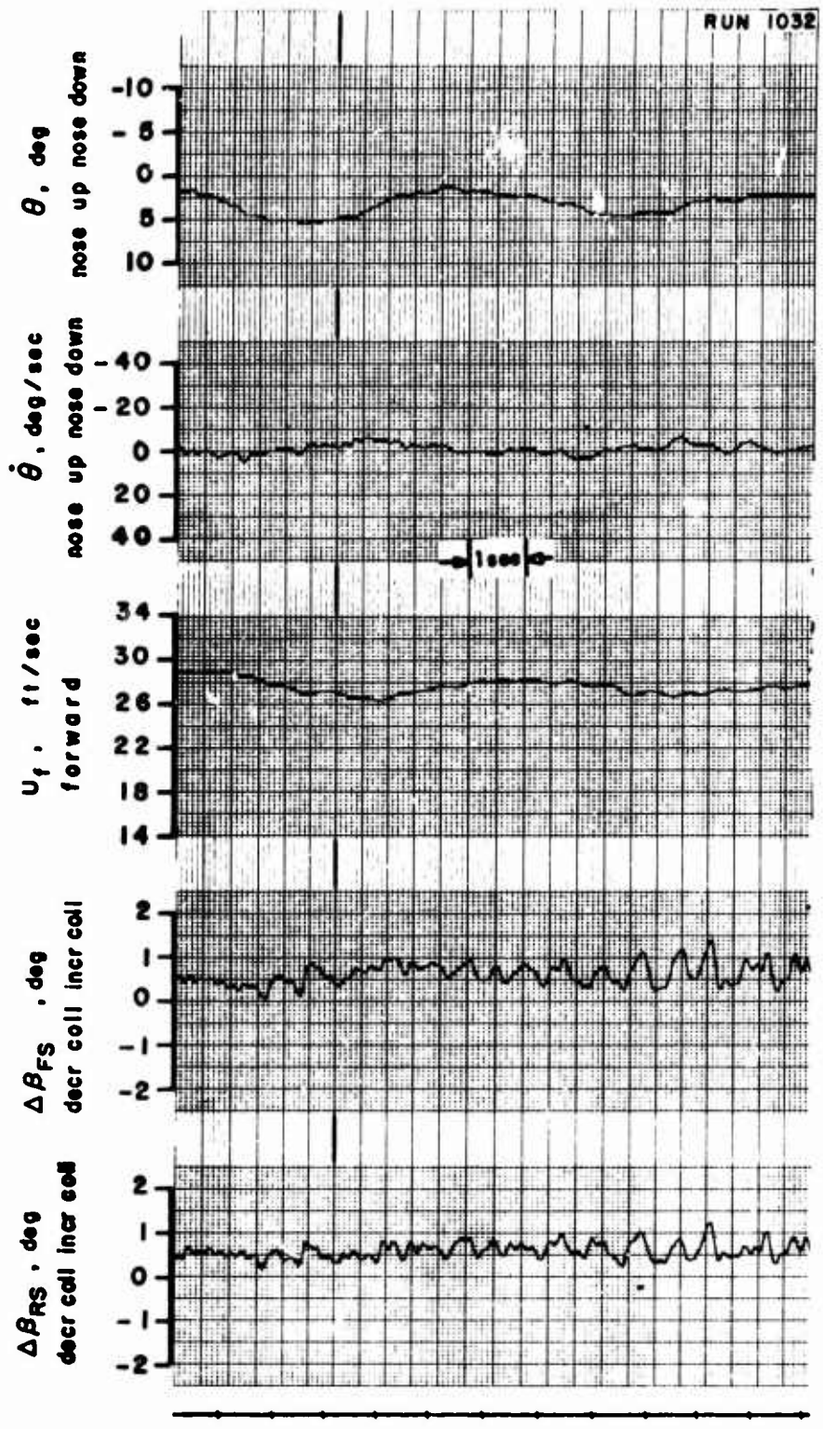

Figure 31. Self-Excited Transient Responses. Two Degrees of Freedom, θ-U_f. $K_{\dot{\theta}}$ = 0.027 sec.
i_d = 60°, $\beta_{.75R}$ = 25.4°, rpm = 6780.

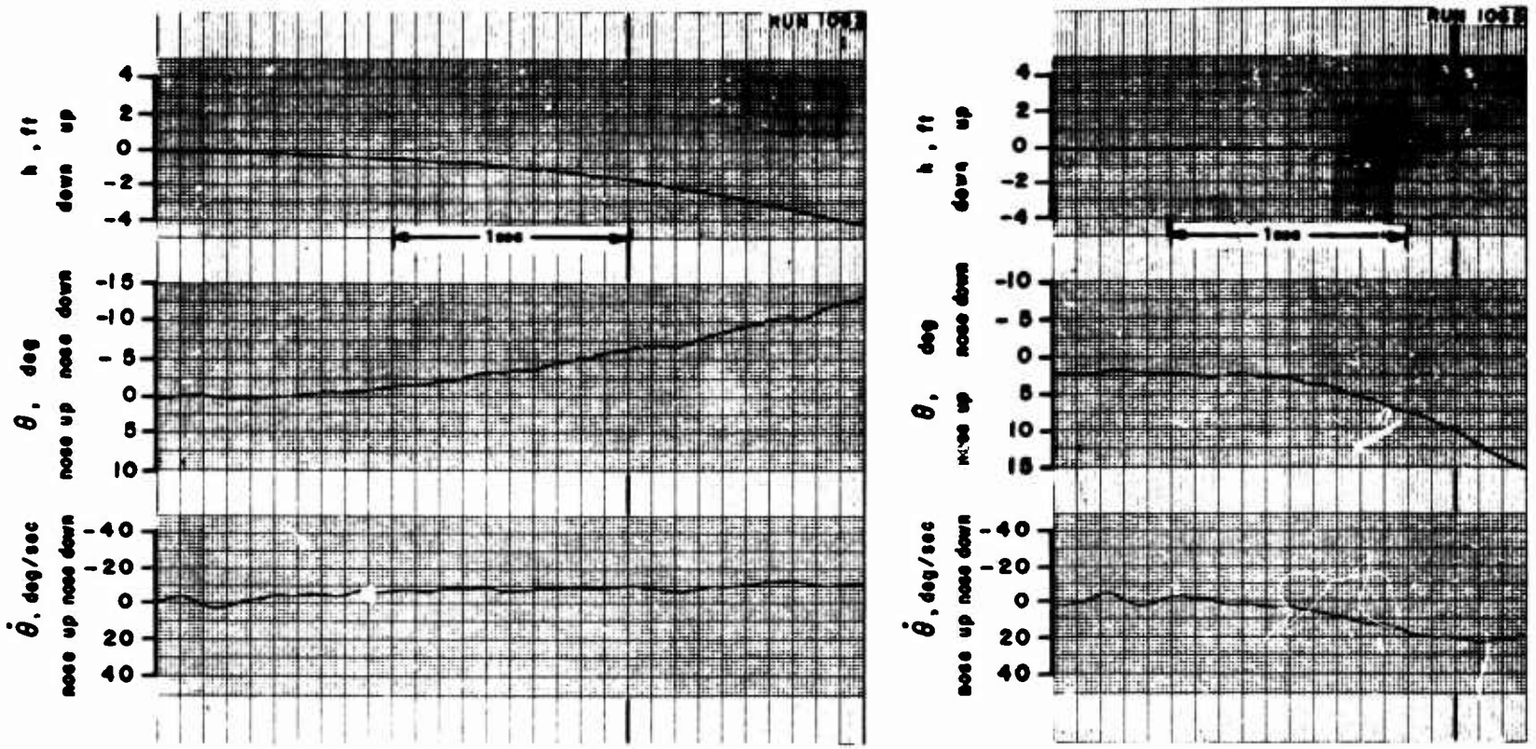

Figure 32. Self-Excited Transient Responses. Two Degrees of Freedom, θ-w_f. No Stability Augmentation.
$i_d = 60°$, $\beta_{.75R} = 25.4°$, rpm = 6780.

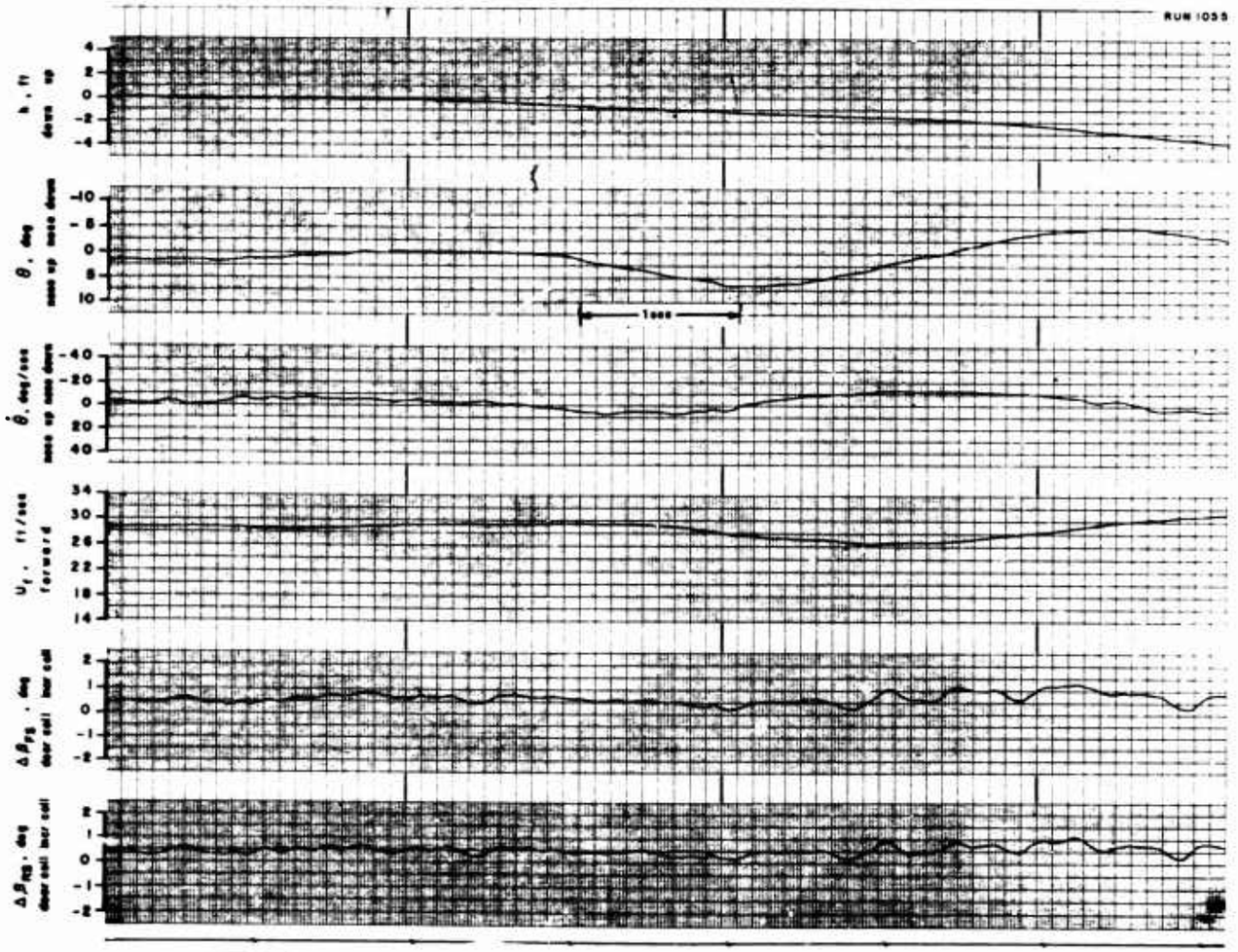

Figure 33. Self-Excited Transient Responses. Three Degrees of Freedom, θ-U_f-w_f. No Stability Augmentation.
$i_d = 60°$, $\beta_{.75R} = 25.4°$, rpm = 6780.

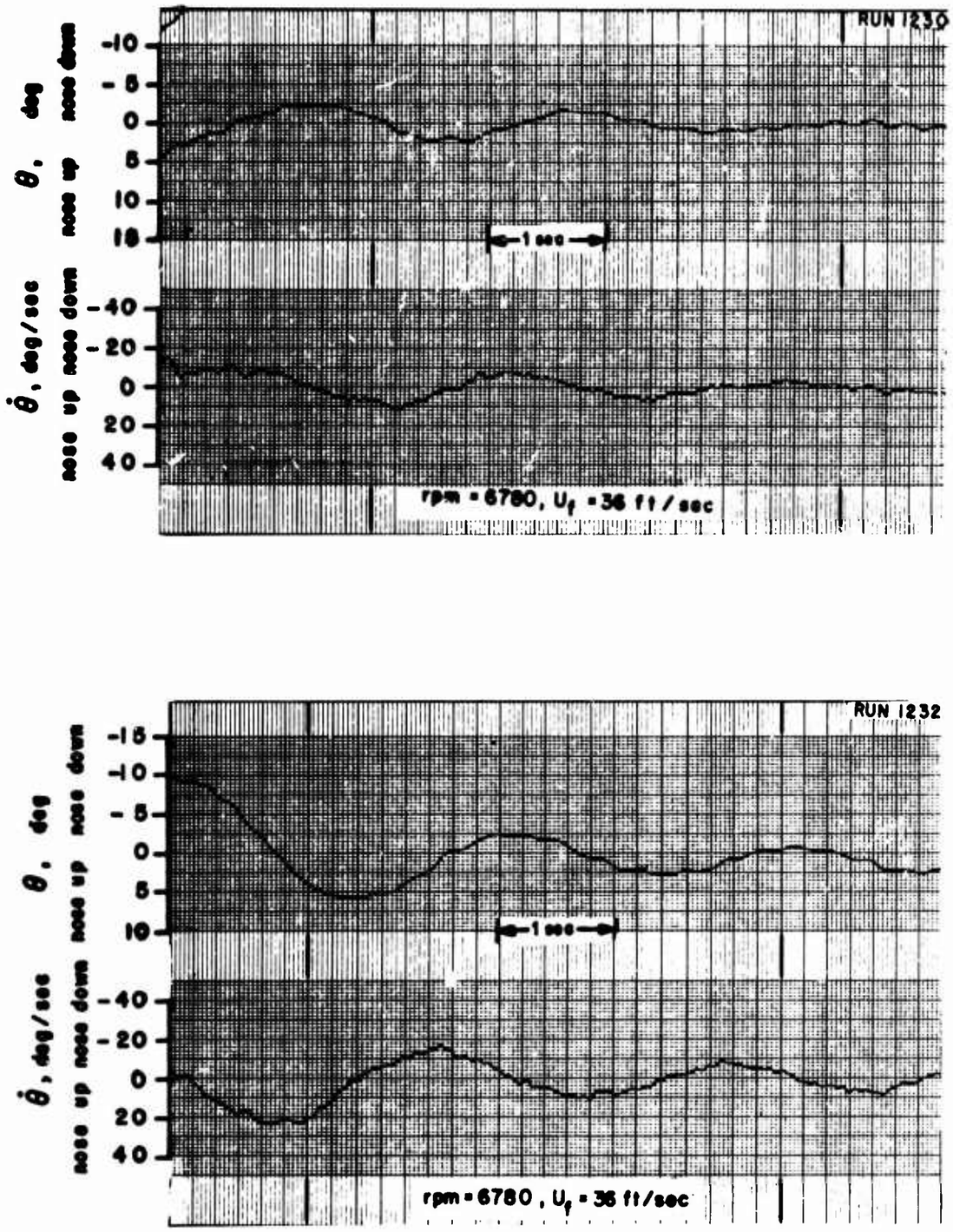

Figure 34. Self-Excited Transient Response. One Degree of Freedom, θ. No Stability Augmentation.
$i_d = 50°$, $\beta_{.75R} = 25.3°$, $U_f = 36$ ft/sec , rpm = 6780.

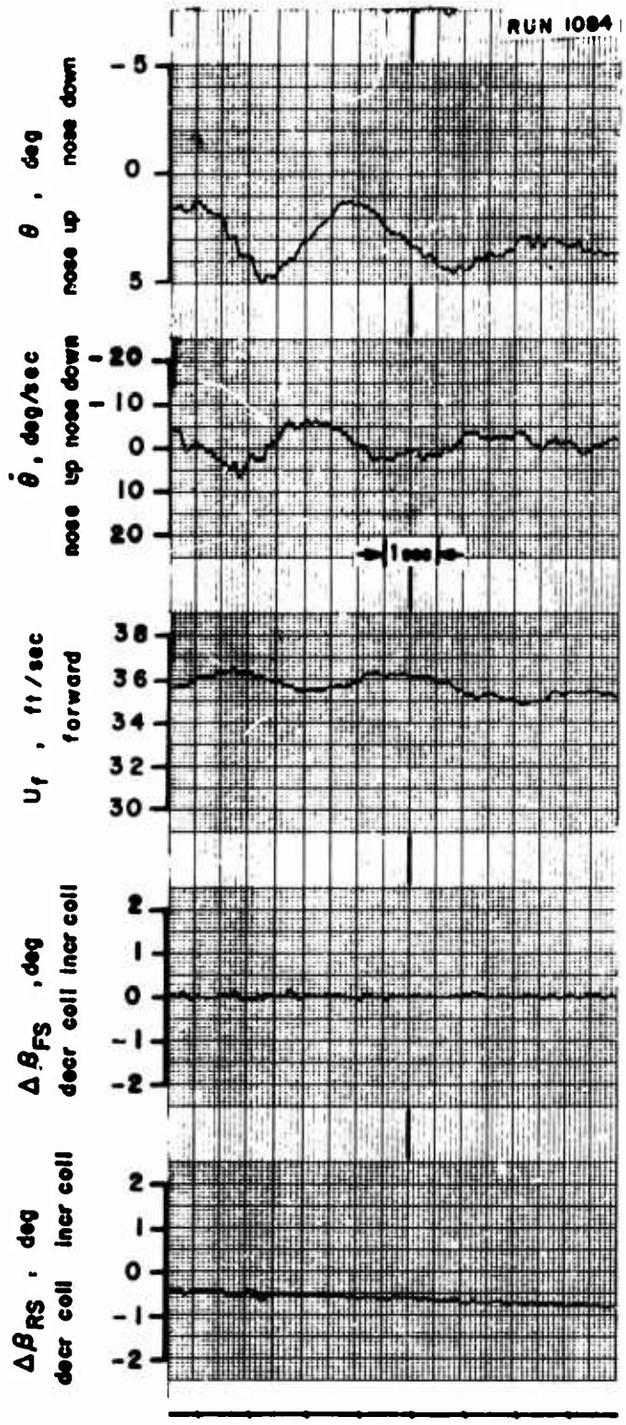

Figure 35. Self-Excited Transient Responses. Two Degrees of Freedom, θ-U_f. No Stability Augmentation.

$i_d = 50°$, $\beta_{.75R} = 25.3°$, rpm = 6780.

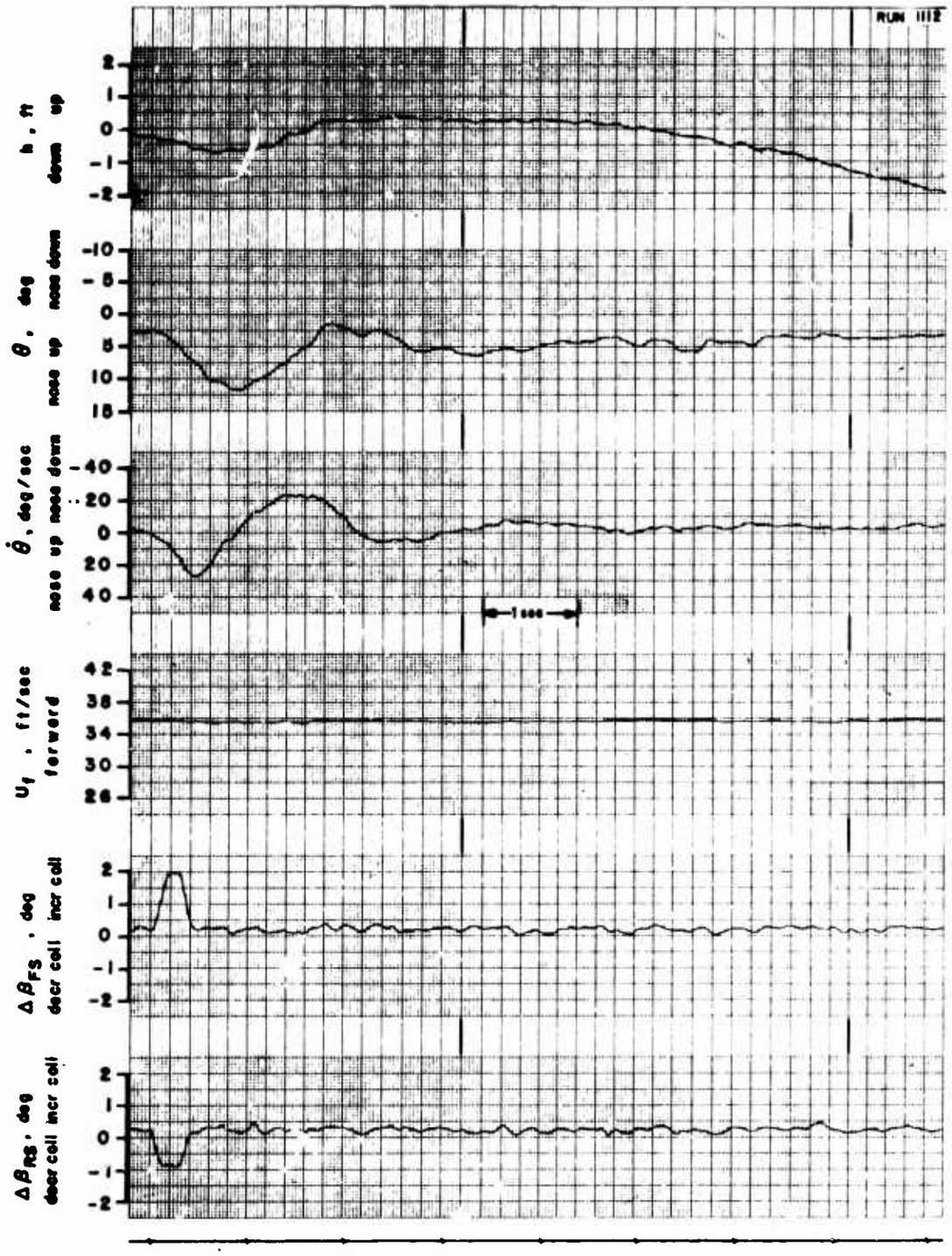

Figure 36. Transient Response to Control Input. Two Degrees of Freedom, θ-w_f. No Stability Augmentation.

$i_d = 50°$, $\beta_{.75R} = 25.3°$, rpm = 6780.

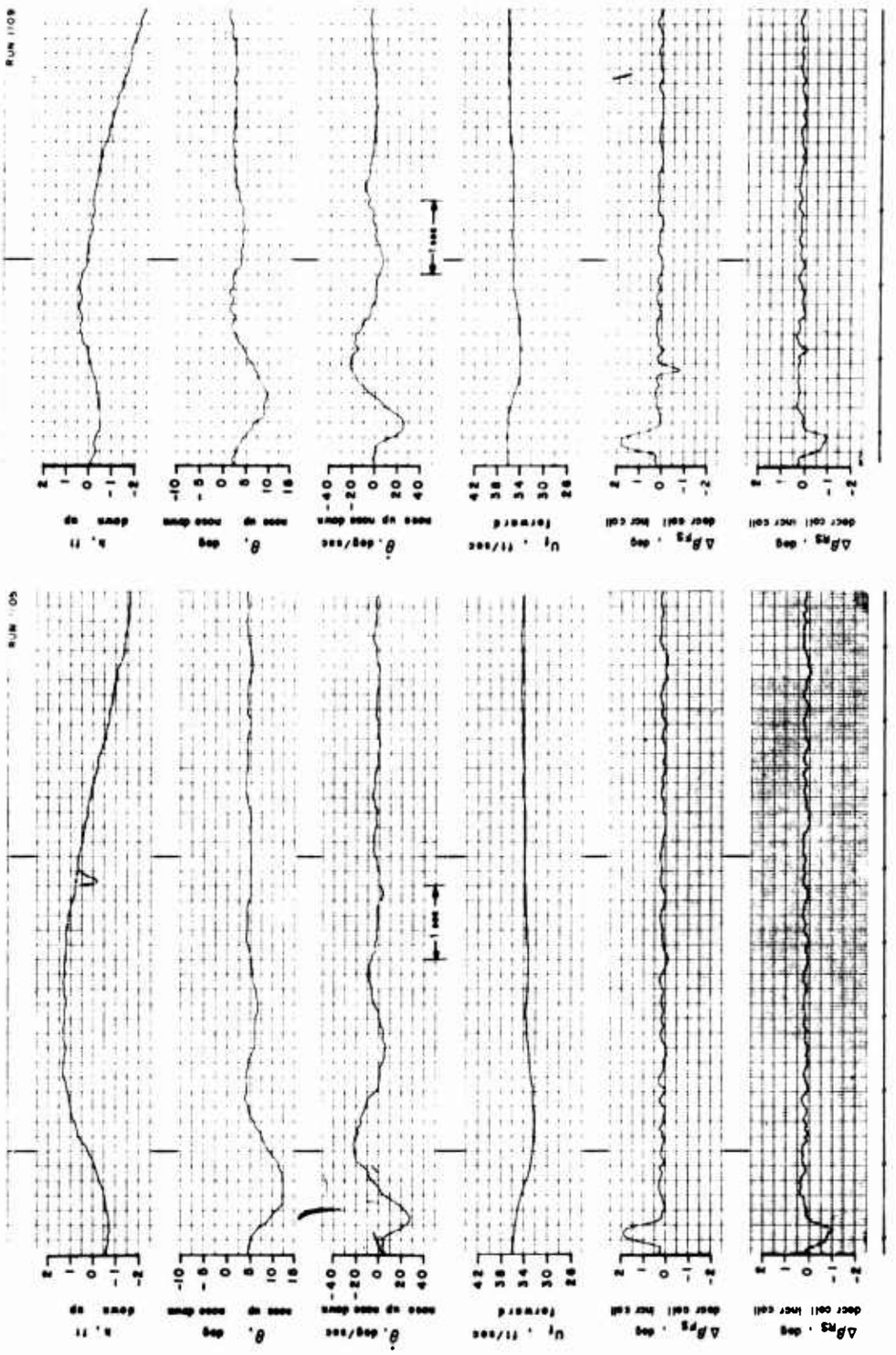

Figure 37. Transient Response to Control Input. Three Degrees of Freedom, θ-U_f-w_f. No Stability Augmentation.
i_d = 50°, $\beta_{.75R}$ = 25.3°, rpm = 6780.

REFERENCES

1. Putman, W. F., Traybar, J. J., Curtiss, H. C., Jr., and Kukon, J. P., AN INVESTIGATION OF THE DYNAMIC STABILITY CHARACTERISTICS OF A QUAD CONFIGURATION, DUCTED-PROPELLER V/STOL MODEL, Princeton University; USAAVLABS Technical Report 68-49A, U. S. Army Aviation Materiel Laboratories, Fort Eustis, Virginia, June 1968.

2. Putman, W. F., SPECIFICATIONS FOR DESIGN OF A VARIABLE CONFIGURATION QUAD MODEL, Princeton University; Department of Aerospace and Mechanical Sciences Report 839, Princeton, New Jersey, October 1965.

3. Michaels, J. L., and Hesby, A. T., AERODYNAMIC STABILITY AND CONTROL AND FLYING QUALITIES, X-22A, Bell Aerosystems Company Report No. 2127-917003, Division of Bell Aerospace Corporation, Buffalo, New York, December 1962.

4. Curtiss, H. C., Jr., Putman, W. F., and Traybar, J. J., GENERAL DESCRIPTION OF THE PRINCETON DYNAMIC MODEL TRACK, Princeton University; USAAVLABS Technical Report 66-73, U. S. Army Aviation Materiel Laboratories, Fort Eustis, Virginia, November 1966, AD 645 883.

5. Seckel, Edward, STABILITY AND CONTROL OF AIRPLANES AND HELICOPTERS, New York, Academic Press, 1964.

APPENDIX
EQUATIONS OF MOTION

Linearized equations of motion, applicable to the analysis of various experimentally measured responses, are presented in this appendix.

The longitudinal equations of motion that describe the small perturbation motion of an aircraft from initially level flight, using a stability axis system (Reference 5) are:

$$\dot{u} - X_u u - X_w w + g\theta = 0$$

$$\dot{w} - Z_w w - Z_u u - U_o \dot{\theta} = 0$$

$$M_w w + M_{\dot{w}} \dot{w} + M_u u + M_{\dot{\theta}} \dot{\theta} - \ddot{\theta} = 0 \qquad (1)$$

Two derivatives $X_{\dot{\theta}}$ and $Z_{\dot{\theta}}$ that are usually small are neglected.

Since all of the transient responses were measured, and are presented in terms of space-fixed variables, it is convenient to transform equations (1) to a space-fixed system, (Figure 38) with the X_f axis parallel to the horizon, by the following transformations:

$$u = u_f - W_{o_f} \theta$$

$$w = w_f + U_{o_f} \theta \qquad (2)$$

where W_{o_f} is equal to zero from the condition of initially level flight.

Substituting relationships (2) into equations (1), the following equations result:

$$\dot{u}_f - X_u u_f - X_w w_f + (g - X_w U_{o_f}) \theta = 0$$

$$\dot{w}_f - Z_w w_f - Z_u u_f - Z_w U_{o_f} \theta = 0$$

$$\ddot{\theta} - (M_{\dot{\theta}} + M_{\dot{w}} U_{o_f}) \dot{\theta} - M_w U_{o_f} \theta - M_u u_f - M_{\dot{w}} \dot{w}_f - M_w w_f = 0 \qquad (3)$$

Because of certain features of the model and the apparatus, three modifications to these equations are necessary such that they will apply to all test conditions.

1. There are two linkages required to attach the model to the servo transducers and mounting system used for this type of testing. These supports provide the horizontal and vertical translational degrees of freedom and contribute additional masses m_h and m_v that "fly" along with the model and therefore, also must be accelerated by the model. The two linkages are relatively small in weight compared to the "flying" weight of the model but nevertheless should be accounted for by additional mass terms in the equations of motion. Generally, the arrangement and weights of these two supports are such that the mass accelerated by the model in the horizontal direction is larger than that accelerated in the vertical direction. If m_p is the total mass of the model resting on the pivot axis (Figure 39), then the total lifted mass of the model m when "flying" is equal to m_p plus the mass of the vertical link m_v or $m = m_p + m_v$. Similarly, the total accelerated mass in the horizontal direction (m_t) is equal to $m_p + m_v + m_h$ or $m + m_h$. This dynamic model-mount characteristic requires the modification of all terms in the horizontal force equation, except the acceleration term, by a mass ratio defined as m/m_t and equal to 0.936 in value.

2. In certain of the test conditions as indicated in Table III, the center of gravity of the model was not located at the pivot axis of the model. Equations (3) may be considered to be written about the pitch pivot axis of the model, which represents the full-scale center-of-gravity position about which the derivatives are determined. Additional terms are necessary in the equations of motion to account for the displacement of the model center of gravity. These are:

$$\Delta M_{\dot{u}_{cg}} = -\frac{z_{cg}\, m_p}{I_y}$$

$$\Delta M_{\dot{w}_{cg}} = \frac{x_{cg}\, m_p}{I_y}$$

$$\Delta M_{\dot{\theta}_{cg}} = -\frac{W_p\, z_{cg}}{I_y} \qquad (4)$$

where m_p and W_p are respectively the pivoting mass and pivoting weight of the model.

3. In certain of the tests (single degree of freedom only) a mechanical spring was added about the model pitch axis to provide a restoring moment which produces an oscillatory motion of the model. In these experiments the following term should be added:

$$\Delta M_{\theta_m} = - \frac{k_{\theta_m}}{I_y} \tag{5}$$

In the experiments where a spring was employed, the value of the spring constant, k_{θ_m}, is given in Table III.

Adding the necessary terms to account for these three effects, the complete equations of motion that apply to the measured transients obtained in this facility are:

$$\dot{u}_f - \frac{m}{m_t} X_u u_f - \frac{m}{m_t} X_w w_f + \frac{m}{m_t} (g - X_w U_{o_f}) \theta = 0$$

$$\dot{w}_f - Z_w w_f - Z_u u_f - Z_w U_{o_f} \theta = 0$$

$$\ddot{\theta} - (M_{\dot{\theta}} + M_{\dot{w}} U_{o_f}) \dot{\theta} + \left(\frac{k_{\theta_m}}{I_y} - M_w U_{o_f} + \frac{W_p z_{cg}}{I_y} \right) \theta + \frac{m_p z_{cg}}{I_y} \dot{u}_f - M_u u_f$$

$$- \left(M_{\dot{w}} + \frac{m_p x_{cg}}{I_y} \right) \dot{w}_f - M_w w_f = 0 \tag{6}$$

For the restricted degree of freedom tests, then the following reduced sets of equations apply.

1. In two degrees of freedom, with $k_{\theta_m} = 0$:

   a. θ, u_f ($w_f = 0$)

$$\dot{u}_f - \frac{m}{m_t} X_u u_f + \frac{m}{m_t} (g - X_w U_{o_f}) \theta = 0$$

$$\ddot{\theta} - (M_{\dot{\theta}} + M_{\dot{w}} U_{o_f}) \dot{\theta} - M_w U_{o_f} \theta$$

$$+ \frac{W_p z_{cg}}{I_y} \theta + \frac{m_p z_{cg}}{I_y} \dot{u}_f - M_u u_f = 0 \tag{7}$$

b. θ, w_f ($u_f = 0$)

$$\dot{w}_f - Z_w w_f - Z_w U_{o_f} \theta = 0$$

$$\ddot{\theta} - (M_{\dot{\theta}} + M_{\dot{w}} U_{o_f}) \dot{\theta} - M_w U_{o_f} \theta$$

$$+ \frac{W_p z_{cg}}{I_y} \theta - \left(M_{\dot{w}} + \frac{m_p x_{cg}}{I_y}\right) \dot{w}_f - M_w w_f = 0 \qquad (8)$$

2. In the single-degree-of-freedom experiments, with the mechanical spring and $u_f = 0$, $w_f = 0$, the equation that applies is:

$$\ddot{\theta} - (M_{\dot{\theta}} + M_{\dot{w}} U_{o_f}) \dot{\theta} + \left(\frac{k_{\theta_m}}{I_y} - M_w U_{o_f} + \frac{W_p z_{cg}}{I_y}\right) \theta = 0 \qquad (9)$$

3. In the experiments where feedback is used, a term $M_{\Delta\beta_{PITCH}} \Delta\beta_{PITCH}$ should be added to the right hand side of the pitching moment equation and then the equation governing $\Delta\beta$ is:

$$\Delta\beta_{PITCH} = K_{\dot{\theta}} \dot{\theta} \qquad (10)$$

By substitution of these expressions into the pitching moment equation, an effective pitch damping is obtained:

$$\bar{M}_{\dot{\theta}} = M_{\dot{\theta}} + K_{\dot{\theta}} M_{\Delta\beta_{PITCH}} \qquad (11)$$

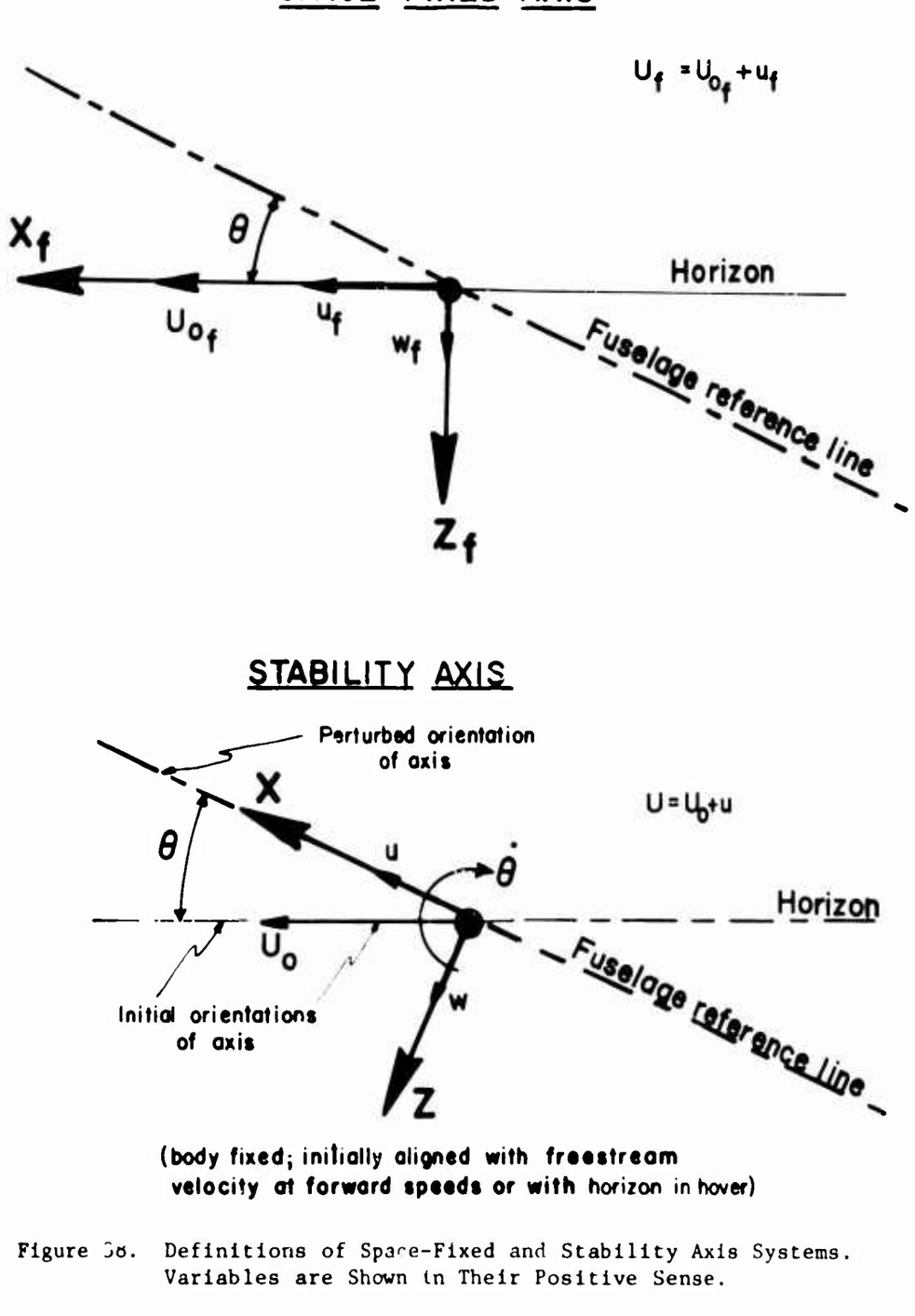

Figure 38. Definitions of Space-Fixed and Stability Axis Systems. Variables are Shown in Their Positive Sense.

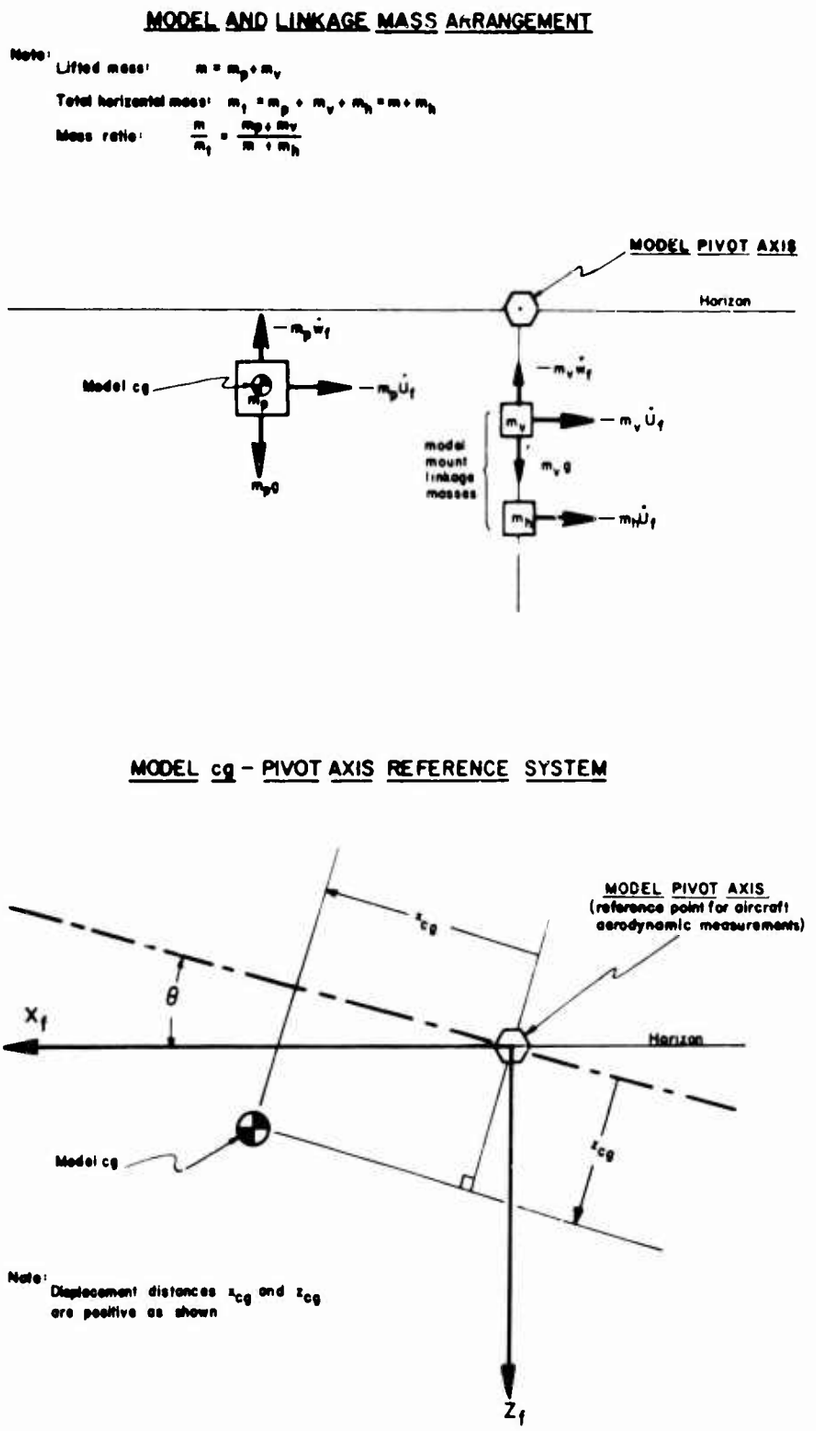

Figure 39. Model and Link Mass Arrangement and Reference System for Model cg-Pivot Axis.

Unclassified

Security Classification

DOCUMENT CONTROL DATA - R & D

(Security classification of title, body of abstract and indexing annotation must be entered when the overall report is classified)

1. ORIGINATING ACTIVITY (Corporate author)	2a. REPORT SECURITY CLASSIFICATION
Princeton University Princeton, New Jersey	Unclassified
	2b. GROUP

3. REPORT TITLE

AN INVESTIGATION OF THE DYNAMIC STABILITY CHARACTERISTICS OF A QUAD CONFIGURATION, DUCTED-PROPELLER V/STOL MODEL
VOLUME II - PHASE II - LONGITUDINAL DYNAMICS AT HIGH DUCT INCIDENCE DATA REPORT

4. DESCRIPTIVE NOTES (Type of report and inclusive dates)

Final Data Report

5. AUTHOR(S) (First name, middle initial, last name)

William F. Putman John P. Kukon
Joseph J. Traybar
Howard C. Curtiss, Jr.

6. REPORT DATE	7a. TOTAL NO. OF PAGES	7b. NO. OF REFS
August 1968	77	5

8a. CONTRACT OR GRANT NO.	9a. ORIGINATOR'S REPORT NUMBER(S)
DAAJ02-67-C-0025	USAAVLABS Technical Report 68-49B
b. PROJECT NO. Task 1F162204A14233	
c.	9b. OTHER REPORT NO(S) (Any other numbers that may be assigned this report)
d.	Aerospace Sciences Report 836

10. DISTRIBUTION STATEMENT

This document has been approved for public release and sale; its distribution is unlimited.

11. SUPPLEMENTARY NOTES	12. SPONSORING MILITARY ACTIVITY
Volume II of a 4-volume report.	US Army Aviation Materiel Laboratories Fort Eustis, Virginia

13. ABSTRACT

The results of experiments to determine the longitudinal dynamic stability characteristics of a quad configuration, ducted-propeller V/STOL aircraft at four low-speed/high-duct-incidence trim conditions (i_d = 80°, 70°, 60°, and 50°) are presented. Longitudinal transient responses in various degrees of freedom were measured using a dynamic model on the Princeton Dynamic Model Track. The data presented include time histories of the model motions in various longitudinal degrees of freedom that occur when the model is disturbed from trimmed flight. Responses are presented both with and without pitch rate feedback.

The dynamic model employed in these experiments is a generalized research model arranged to represent closely the ~~Bell~~ X-22A V/STOL aircraft.

The data presented in this report comprise the second phase of a three-phase investigation of the dynamic stability characterisitics of a quad configuration, ducted-propeller V/STOL aircraft at low speeds and high duct incidences. The other two phases pertain to the lateral and longitudinal hovering stability characteristics, presented in Reference 1, and the lateral/directional characteristics at the same trim conditions as presented here.

DD FORM 1 NOV 68 1473 REPLACES DD FORM 1473, 1 JAN 64, WHICH IS OBSOLETE FOR ARMY USE.

Unclassified

Security Classification

14. KEY WORDS	LINK A		LINK B		LINK C	
	ROLE	WT	ROLE	WT	ROLE	WT
V/STOL						
Dynamic Stability						
Longitudinal Stabilities						
Transient Response						
Bell X-22A						
Hovering Characteristics						